

Discovery of Pyridazinopyridinones as Potent and Selective p38 Mitogen-Activated Protein Kinase Inhibitors

Bin Wu,^{*,†} Hui-Ling Wang,[†] Liping Pettus,[†] Ryan P. Wurz,[†] Elizabeth M. Doherty,[†] Bradley Henkle,[‡] Helen J. McBride,[‡] Christiaan J. M. Saris,[‡] Lu Min Wong,[‡] Matthew H. Plant,^{||} Lisa Sherman,[‡] Matthew R. Lee,[§] Faye Hsieh,[#] and Andrew S. Tasker[†]

[†]Department of Chemistry Research and Discovery, [‡]Inflammation, ^{||}HTS Molecular Pharmacology, [§]Molecular Structure, and [#]Pharmacokinetics and Drug Metabolism, Amgen Inc., One Amgen Center Drive, Thousand Oaks, California 91320

Received May 10, 2010

The p38 mitogen-activated protein kinase (MAPK) plays an important role in the production of proinflammatory cytokines, making it an attractive target for the treatment of various inflammatory diseases. A series of pyridazinopyridinone compounds were designed as novel p38 kinase inhibitors. A structure–activity investigation identified several compounds possessing excellent potency in both enzyme and human whole blood assays. Among them, compound **31** exhibited good pharmacokinetic properties and showed excellent selectivity against other related kinases. In addition, **31** demonstrated efficacy in a collagen-induced arthritis disease model in rats.

Introduction

The p38 mitogen-activated protein (MAP)^a kinases are major components of the MAP kinase pathway that transduces extracellular signals to intracellular responses.¹ There are four isoforms in the p38 family, referred to as α , β , γ , and δ , with differential expression and activation patterns.² Of the four known isoforms, p38 α is considered to be the most relevant kinase involved in the inflammatory response. Upon activation by extracellular stress stimuli, p38 activates several downstream kinases (i.e., MK2, MK3) and transcription factors (i.e., Stat1, ATF-2) and plays an essential role in the production of proinflammatory cytokines such as IL-1 β , TNF α , and IL-6.³ It is known that therapeutics that block the production of these cytokines provide relief of the symptoms of a variety of inflammatory diseases.⁴ Thus, p38 is an attractive target for the treatment of rheumatoid arthritis (RA), chronic obstructive pulmonary disease (COPD), and psoriasis, and as such has been the subject of intense research within the pharmaceutical industry since its discovery in the early 1990s.⁵

We recently reported the discovery of a series of potent ATP-competitive p38 inhibitors typified by the phthalazine **1** (p38 α IC₅₀ = 0.8 nM) and pyrazolopyridinone **2** (p38 α IC₅₀ = 3.2 nM) that exploit features of the ATP binding site unique to p38 α (Figure 1).⁶ X-ray cocrystal structures revealed that both **1** and **2** bind to p38 α in the so-called DFG-in mode, in which Phe169 of the DFG-motif is buried in its highly conserved cognate hydrophobic pocket.^{7,8} As shown in Figure 2, the methyl groups on the toluamide rings of **1** and **2** occupy

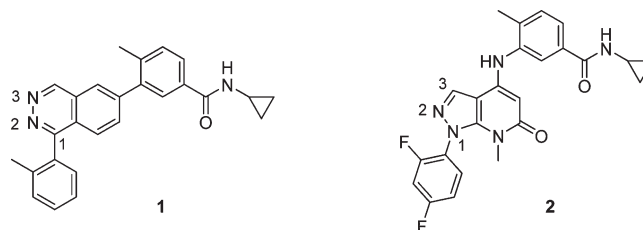


Figure 1. Phthalazine and pyrazolopyridinone as p38 inhibitors.

a hydrophobic pocket defined by the residues Thr106, Leu104, and Lys53. The cyclopropyl amide of those inhibitors forms polar interactions with Asp168 and Glu71. The phthalazine of **1** engages the strand that connects the N- and C-terminal domains, referred to as the “linker strand”. Both N-2 and N-3 of the phthalazine function as hydrogen bond acceptors to the linker strand, one through a classical interaction with Met109, seen in all ATP-competitive kinase inhibitors, and the second with Gly110, which is flipped when compared to classical kinase inhibitors.⁹ The tolyl ring at C-1 forms a series of van der Waals contact with the backbone of the linker strand, while the tolyl methyl group tightly fills a small hydrophobic cavity on the floor of the binding site, defined by Ala157 and Leu104. According to the multiple sequence alignment used in the widely recognized analysis of the human kinome in 2002 by Manning et al.,¹⁰ an alanine residue in this floor region of the active site is common to only three other protein kinases (TTBK1, TTBK2, and TSSK3) outside of the p38 family (with no kinases having the smaller glycine), so it is reasoned that the interaction with this residue is the basis for the high selectivity of these agents. Finally, the hydrophobic benzenoid ring of the phthalazine in **1** engages in an edge-to-face interaction with Tyr35 from the tip of the P-loop. In compound **2**, N-2 of the pyrazolopyridinone forms a hydrogen bond with the backbone NH of Met109, while the

*To whom correspondence should be addressed: Tel 805-313-5661; fax 805-480-3016; e-mail: binw@amgen.com.

^aAbbreviations: MAP, mitogen-activated protein; RA, rheumatoid arthritis; COPD, chronic obstructive pulmonary disease; DFG, Asp-Phe-Gly sequence in ATP binding site; hWB, human whole blood; THP1, human acute monocytic leukemia cell line; PMB, *para*-methoxy benzyl; DIBAL, diisobutyl aluminum hydride; LAH, lithium aluminum hydride; AUC, area under curve.

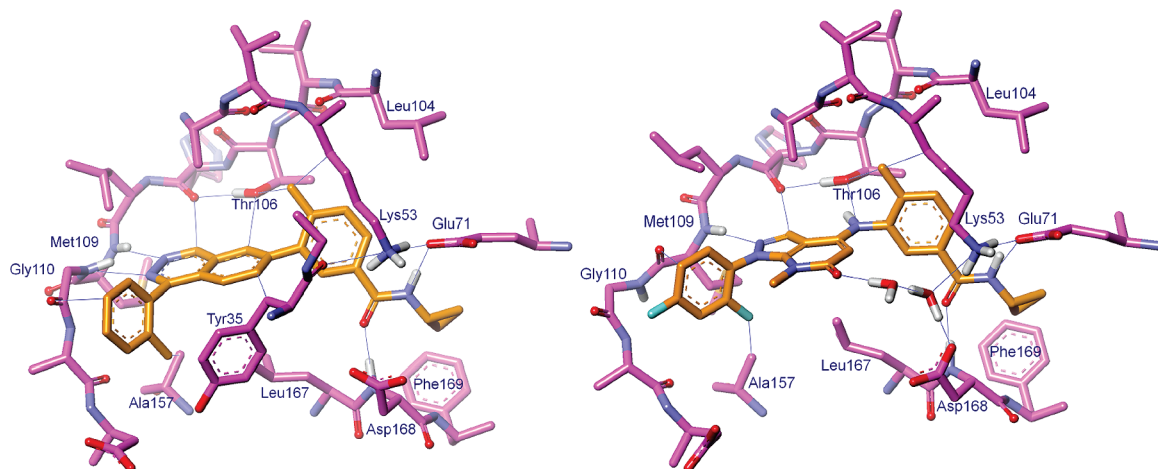
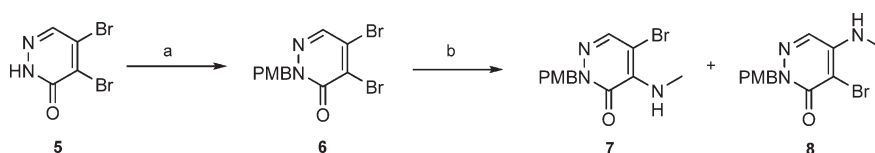


Figure 2. Co-crystal structures of compounds **1** and **2** with unphosphorylated p38 α .

Scheme 1. Selective Amination of 4,5-Dibromopyridazinone^a



^a Reagents and conditions: (a) PMBCl, K₂CO₃, Bu₄NBr, MeCN, 60 °C, 60%; (b) MeNH₂, toluene, microwave, 100 °C, 81%.

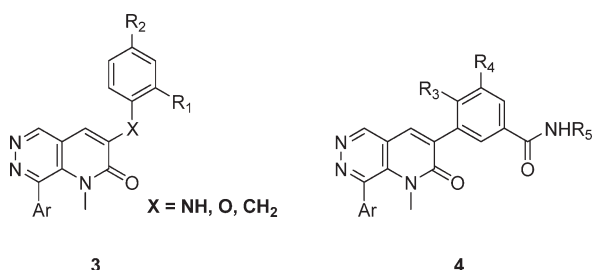
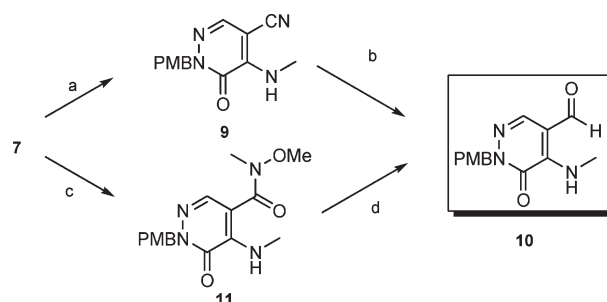


Figure 3. Pyridazinopyridinones as p38 inhibitors.

ortho fluoro substituent is directed downward in a low energy conformation, orthogonal to the pyrazolopyridinone ring, to form a well-defined hydrophobic contact with Ala157. In contrast to compound **1**, the P-loop maintains an extended conformation, in which the Tyr35 residue (not shown) lies 7 Å from the polar pyridinone carbonyl, separated by two crystallographically resolved water molecules, which also form a network of hydrogen bonds involving the carbonyl of compound **2** and the charged side chain termini of Asp168 and Lys53.

While **1** and **2** demonstrated excellent potency in enzyme assays and selectivity against other kinases, they suffered from unfavorable pharmacokinetic properties such as moderate clearance (**1**: Cl 1.7 L/h/kg) and low bioavailability (**2**: F 12%). Consequently, as part of our continuing efforts to pursue selective p38 inhibitors for the treatment of inflammatory diseases, we designed pyridazinopyridinone analogues **3** and **4**, by merging key elements of compounds **1** and **2** to further exploit the unique features of the ATP binding site of p38 α (Figure 3). The goal of these novel inhibitors was to improve the pharmacokinetic liabilities while retaining the favorable pharmacological properties of the previous series. Herein, we describe the synthesis, structure–activity relationships (SAR), pharmacokinetics, and in vivo pharmacology of these new classes of compounds.

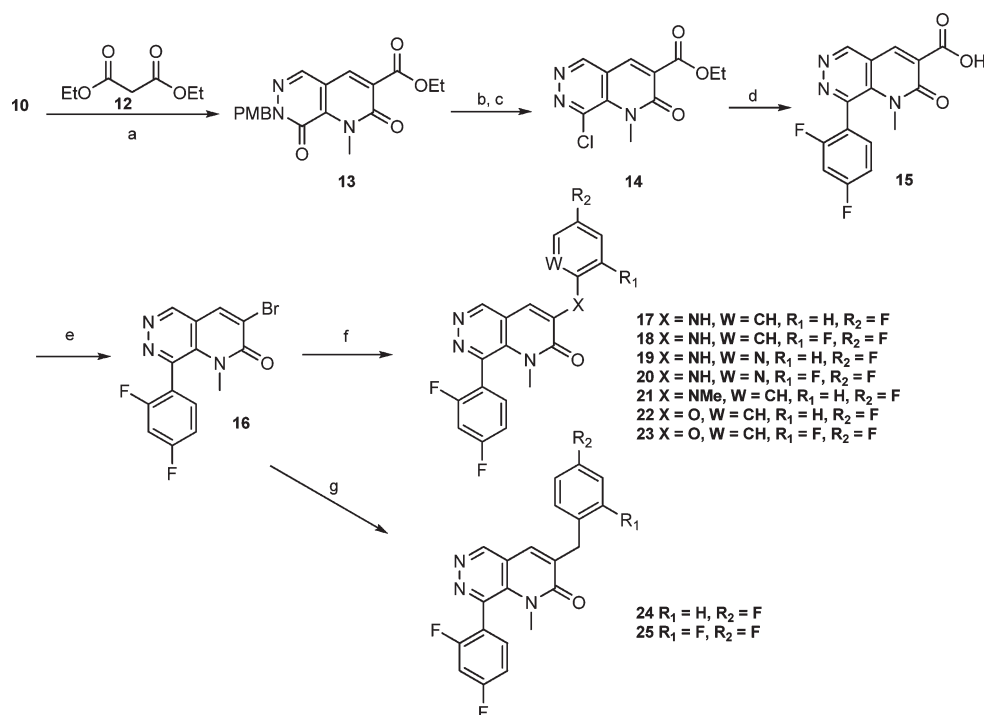
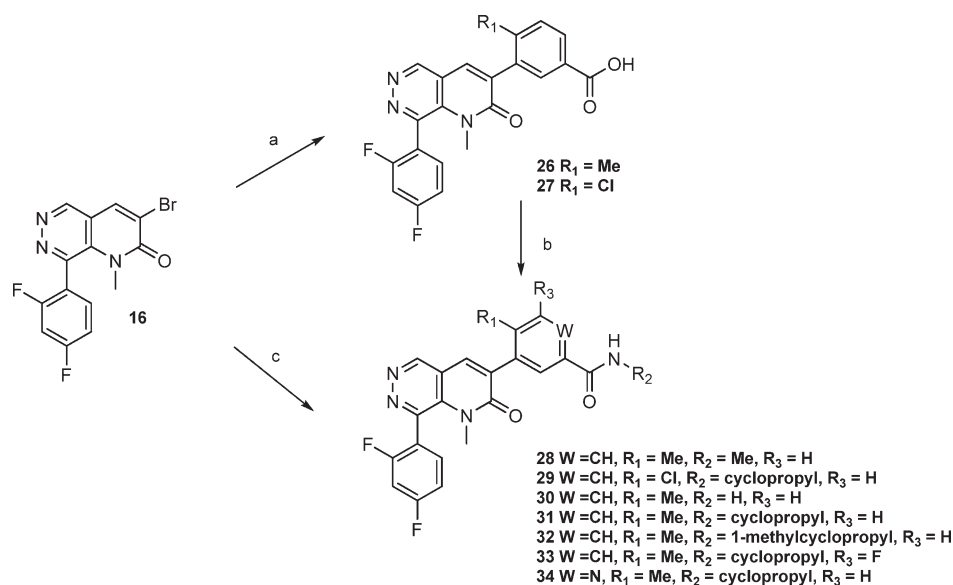
Scheme 2. Synthesis of Aldehyde Intermediate **10**^a



^a Reagents and conditions: (a) CuCN, DMF, microwave, 200 °C, 94%; (b) DIBAL, THF, 0 °C, 59%; (c) CO (30 psi), Pd(OAc)₂, XantPhos, MeNH(OMe), toluene, 110 °C, 64%; (d) LAH, THF, 100%.

Chemistry

The synthesis of the pyridazinopyridinone series commenced with 4,5-dibromo-pyridazinone (**5**, Scheme 1). *N*-Protection of **5** with a *p*-methoxybenzyl group followed by treatment with methylamine in *p*-dioxane led to a mixture of regioisomers with a 2:1 ratio, favoring the desired 5-bromo-4-(methylamino)pyridazin-3(2H)-one **7**. It is well documented that, in nucleophilic substitutions of 4,5-dihalo-pyridazin-3(2H)-one, the solvent plays an important role in the product distribution.¹¹ By switching to toluene as the solvent, the ratio of regioisomers **7** to **8** was improved to >5:1. The subsequent cyanation of **7** with copper cyanide under microwave irradiation led to **9**, which was reduced to aldehyde **10** with diisobutyl aluminum hydride (DIBAL) (Scheme 2). Alternatively, intermediate **10** was also prepared through Weinreb amide **11** in a two-step sequence which proved more amenable to large-scale production. Palladium-catalyzed aminocarbonylation generated the Weinreb amide **11**,¹² which was subsequently converted to **10** by lithium aluminum hydride (LAH) reduction.

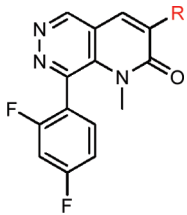
Scheme 3. Preparation of Pyridazinopyridinone Analogues **17–25**^a**Scheme 4.** Synthesis of Pyridazinopyridinone Analogues^a

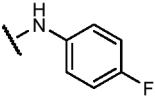
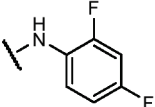
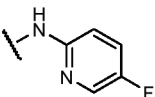
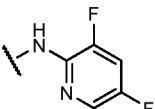
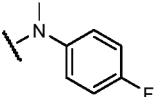
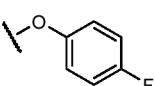
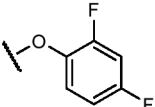
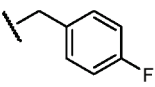
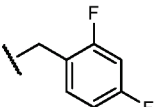
^a Reagents and conditions: (a) 3-borono-4-methylbenzoic acid or 3-borono-4-chlorobenzoic acid, Pd(PPh₃)₄, Na₂CO₃, dioxane/H₂O (4:1); (b) MeNH₂ or cyclopropylamine, HATU, DIPEA, DMSO; (c) ArB(OR)₂, Pd(PPh₃)₄, Na₂CO₃, microwave, dioxane/H₂O (4:1).

As shown in Scheme 3, cyclocondensation of **10** with diethyl malonate (**12**) in the presence of piperidine furnished pyridazinonepyridinone **13**.¹³ The *p*-methoxybenzyl (PMB) protecting group was then removed by TFA, and treatment of the resulting pyridazinone with POCl₃ yielded aryl chloride **14**, a common intermediate for both series. Suzuki coupling reaction of **14** with 2,4-difluorophenyl boronic acid, followed by saponification of the ester, yielded carboxylic acid **15**. The subsequent decarboxylative bromination, according to Chowdhury et al.,¹⁴ afforded aryl bromide **16**. Pyridazinopyridinones **17–23** were

obtained through Buchwald-Hartwig coupling with the corresponding anilines or phenols, and analogues **24** and **25** were prepared by Negishi coupling with the alkyl zinc reagents.¹⁵

Alternatively, Suzuki reaction of intermediate **16** with 2-methyl-5-carboxyphenylboronic acid or 2-chloro-5-carboxyphenylboronic acid followed by amide formation yielded compound **28** and **29** (Scheme 4). Analogues **30–34** were generated through Suzuki coupling reaction with the corresponding boronic esters with the amide already installed.¹⁶

Table 1. SAR: Pyridazinopyridinones 17–25^a


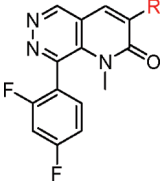
compound	R	p38 α IC ₅₀ (nM)	THP1/TNF α IC ₅₀ (nM)	hWB TNF α /IL8 IC ₅₀ (nM)
17		2.2 \pm 0.2	13.7 \pm 2.3	61.9 \pm 31.4
18		0.9 \pm 0.3	4.5 \pm 1.2	11.7 \pm 4.8
19		328 \pm 200	>2500 ^b	>2500 ^b
20		111 \pm 24	982 \pm 256	>2500 ^b
21		299 \pm 22	1145 \pm 273	1237 \pm 589
22		78 \pm 68	235 \pm 34	227 \pm 68
23		8.4 \pm 1.9	107 \pm 21	70.5 \pm 43.1
24		55.8 \pm 3.2	197 \pm 4	697 \pm 424
25		6.1 \pm 0.2	49 \pm 15	213 \pm 109

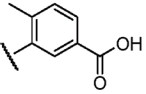
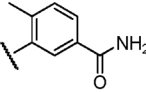
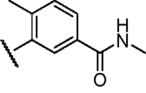
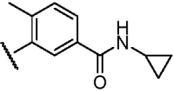
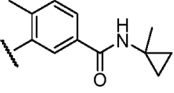
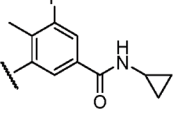
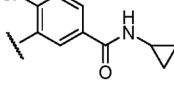
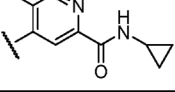
^a Standard deviations are given when $n \geq 3$. ^b Average of two measurements.

Results and Discussion

In Vitro SAR. Compounds were evaluated for their ability to inhibit the phosphorylation of substrate activating transcription factor 2 (ATF2) by recombinant human p38 α . In parallel, the inhibition of LPS-induced

TNF α production in THP1 cells and TNF-induced IL-8 production in human whole blood was measured. The results shown in Tables 1–3 are based on the average of at least three independent experiments, unless noted otherwise, and are reported as IC₅₀ with standard deviation.

Table 2. SAR: Toluamide Ring^a


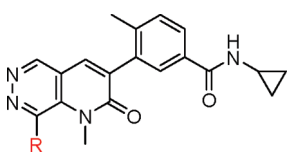
compound	R	p38 α IC ₅₀ (nM)	THP1/TNF α IC ₅₀ (nM)	hWB TNF α /IL8 IC ₅₀ (nM)
26		>1000 ^b	>2500 ^b	>2500 ^b
30		2.7 \pm 0.8	19.3 \pm 5.0	21.3 \pm 11.5
28		2.7 \pm 1.0	24.3 \pm 8.3	30.0 \pm 4.8
31		2.7 \pm 0.8	2.1 \pm 0.4	1.8 \pm 0.5
32		3.1 \pm 0.5	14.5 \pm 2.7	27.4 \pm 9.8
33		1.4 \pm 0.5	1.1 \pm 0.1	1.6 \pm 0.4
29		2.6 \pm 0.4	6.3 \pm 2.3	8.3 \pm 2.6
34		14.5 \pm 3.4	80.5 \pm 27.6	63.3 \pm 30.9

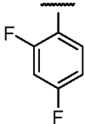
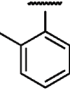
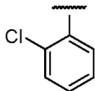
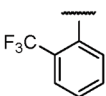
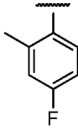
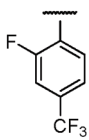
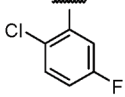
^a Standard deviations are given when $n \geq 3$. ^b Average of two measurements.

Analogues of pyridazinopyridinone represented by generic structure **3** (Figure 3), in which the aromatic ring was attached to the pyridinone ring at the 3 position via N, O, or CH₂ linkage, were evaluated first (Table 1). The 4-fluoroaniline analogue **17** showed good potency, and adding one more fluorine atom in the ortho position of the aniline (**18**) further improved the potency by 5-fold in the whole blood assay. In contrast, replacement of the phenyl with a pyridine (i.e., **19** and **20**) likely led to a stabilization of the small molecule conformational preference away from the binding mode and methylation of the amine (**21**) likely led to an unfavorable interaction with the protein; both resulted in substantial loss of activity.

Similarly, replacement of the linker -NH with either -O or -CH₂ also led to a loss in activity (**22**, **24**, vs **17**), although this could be somewhat rescued by the introduction of a second fluorine atom at the ortho position (**23** and **25**). Molecular

modeling of compound **17** in the ATP binding site of unphosphorylated p38 α suggested that, as in the case of the cocrystal with compound **2**, ligand binding was water mediated, albeit through a single, highly ordered water molecule rather than multiple water molecules. In the model of **17**, as illustrated in Figure 4, the coordinated water molecule was completely shielded from bulk solvent with both hydrogens held in place by hydrogen bonds with the carbonyl on **17** and the carboxylate on Asp168 as well as both oxygen lone pairs held in place by hydrogen bonds with the anilinic NH of **17** and the primary amine of Lys53. With *O*-linked analogues (**22**, **23**), the coordinated water molecule would experience a much less favorable environment. The NH to O change presents one less hydrogen bond donor and one additional hydrogen bond acceptor, leaving the bound water molecule in the presence of three hydrogen bond acceptors and one donor, a significant difference expected

Table 3. SAR: C(8) Substitution^a


compound	R	p38 α IC ₅₀ (nM)	THP1/TNF α IC ₅₀ (nM)	hWB TNF α /IL8 IC ₅₀ (nM)
31		2.7 \pm 0.8	2.1 \pm 0.4	1.8 \pm 0.5
35		2.7 \pm 1.0	1.9 \pm 1.1	1.1 \pm 0.2
36		2.1 \pm 0.5	1.2 \pm 0.3	1.7 \pm 0.02
37		3.9 \pm 0.9	5.5 \pm 1.7	4.3 \pm 1.6
38		3.1 \pm 1.2	2.7 \pm 0.9	2.3 \pm 0.8
39		2.9 \pm 0.7	7.7 \pm 2.2	7.3 \pm 1.5
40		1.6 \pm 0.6	2.0 \pm 0.7	2.2 \pm 1.1

^a Standard deviations are given when $n \geq 3$.

to result in electrostatic repulsion for one of the water molecule oxygen lone pairs. This likely accounts for the 10–40 fold reduction in potency of these analogues. In the case of the CH₂-linked series (**24**, **25**), the water molecule would be surrounded by two hydrogen bond acceptors and one donor, leaving one of the water molecule's oxygen lone pair desolvated by the nonpolar aliphatic carbon. In addition, the strong bias for a tetrahedral geometry of the sp³ methylene spacer would impart a significant penalty upon binding to the protein, creating internal strain of the kinase inhibitor to adopt the same binding mode. While the desolvation penalty of the coordinated water molecule was likely not as significant as with the O-linkage, the ligand's internal strain penalty was greater; taken together, these two factors likely accounted for the 7–25 fold reduction in potency associated with the CH₂-linkage that was comparable to the 10–40 fold loss imparted by the O-linkage. The model of a tightly bound water molecule also is consistent with the ~100 fold loss of potency resulting from N-methylation of the anilinic amine (**21**), as previously alluded to.

On the basis of its excellent potency in the whole blood assay (IC₅₀ = 12 nM), compound **18** was then profiled for its pharmacokinetic parameters in male Sprague–Dawley rats. **18** displayed moderate plasma clearance and half-life (Cl = 1.42 L/h/kg and $t_{1/2}$ = 2.79 h), but low oral bioavailability F (5%). In light of this unfavorable pharmacokinetic profile and the generally poor potency of the linker series in whole blood assays, we turned our attention to the analogues represented by the generic structure **4**.

The preliminary SAR study of these analogues, in which the aromatic ring is directly attached to the pyridone at the 3 position, is shown in Table 2. As anticipated based on our previous SAR, carboxylic acid **26** was devoid of activity, presumably due to a repulsive electrostatic interaction with Glu71 located on the C α -helix of the enzyme. In contrast, the primary amide **30** was potent in all three assays with IC₅₀ values of 2.7, 19, and 21 nM in the enzyme, THP1 cell, and whole blood assays, respectively. Further extension of the amide from methyl, to cyclopropyl and

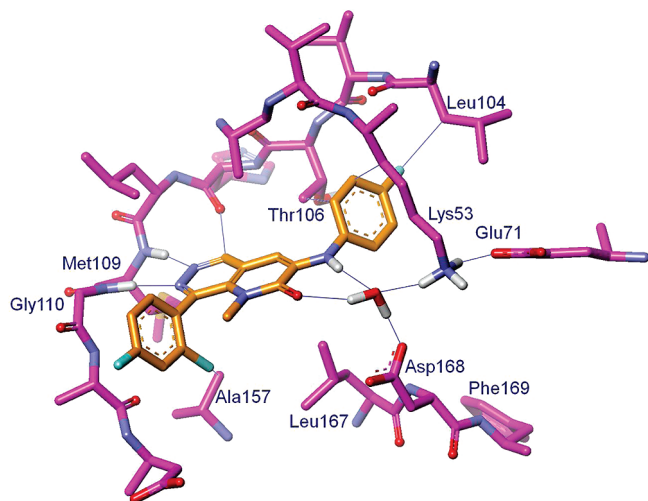


Figure 4. Molecular model of compound **17** in the ATP binding site of unphosphorylated p38 α .

1-methylcyclopropyl (compounds **28**, **31**, **32**, respectively), had little impact on enzyme activity, but afforded an improvement in cell activity in the case of cyclopropyl (**31**). We then looked at substitution of the aromatic ring. Replacement of 4-methyl with 4-chloro (compare **29** to **31**) was well tolerated as was the introduction of the fluoro atom at C5 (**33**). The pyridine analogue **34**, however, was less potent in all assays with over 30-fold reduction in the whole blood assay compared with **31**, again presumably due to an unfavorable electrostatic interaction with Glu71, the loss of a van der Waals interaction with Leu75, or both.

By keeping the toluamide constant as cyclopropylbenzamide and we then turned our attention to substitution at C(8) of the pyridazinopyridinone (Table 3). The strategy here was to maintain, minimally, an ortho substituent to ensure a 90° torsion to engage Ala157 and hopefully clash with the more common Leu/Met residues from other protein kinases, while examining the impact of different functional groups on potency and pharmacokinetics. Compounds **35**–**40** were prepared in a manner similar to compound **31**. As shown in Table 3, replacement of the 2-fluoro with 2-methyl, 2-chloro, or 2-trifluoromethyl as well as replacement of the 4-fluoro substituent with 4-trifluoromethyl resulted in no significant change in activity across enzyme, cell and whole blood assays. In addition, a 5-fluoro substitution was well tolerated.

Molecular modeling of compound **31** in the ATP binding site of unphosphorylated p38 α suggested that, similar to compound **17**, N-6 and N-7 of the pyridazinopyridinone form hydrogen bonds with NH of Met109 and NH of the flipped Gly110, respectively, while a water molecule forms a hydrogen bond network with the carbonyl of the pyridazinopyridinone, Asp168, Ala34, and Lys53 (Figure 5). The methyl group on the toluamide ring was placed in the hydrophobic gatekeeper pocket and the cyclopropylamide positioned to engage with Glu71 and Asp168 through two polar interactions, analogous to the interactions observed in the cocrystal of compound **1** and p38 α (Figure 2). In addition, the model positioned the 2,4-difluorophenyl ring tightly between Ala157 and Leu167 below the plane of pyridazinopyridinone.

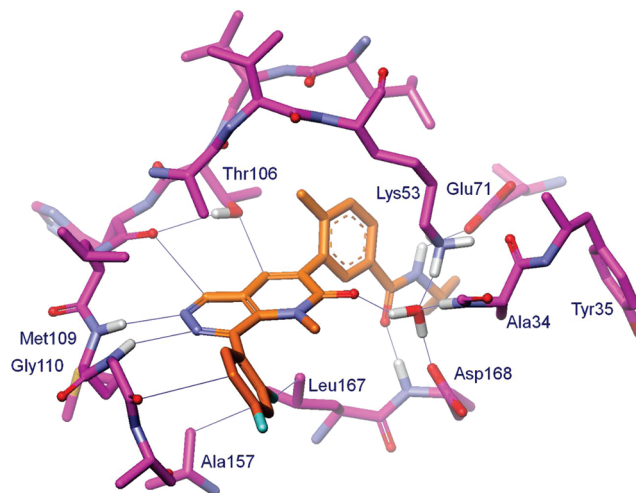


Figure 5. Molecular model of compound **31** in the ATP binding site of unphosphorylated p38 α .

Table 4. In Vitro Pharmacokinetic Profile of Compounds **31**, **33**, **35**, **36**, and **38**

compound	iv (2.0 mg/kg in DMSO) ^a			po (2.0 mg/kg) ^{a,b}	
	CL (L/h/kg)	Vdss (L/kg)	t _{1/2} (h)	AUC (ng·h/mL)	F (%)
31	0.23	1.04	3.06	7633	86
33	0.30	1.19	4.66	6737	55
35	4.91	2.09	2.15	543	132
36	0.79	1.65	2.73	1460	57
38	1.84	1.73	3.35	2410	116

^aValues are the average of 3 runs. ^bVehicle: 1% Pluronic F68, 1% HPMC, 15% hydroxypropyl β -cyclodextrin, 83% water.

Pharmacokinetic Profile and Kinase Selectivity

On the basis of their whole blood potency, selected compounds were further evaluated in pharmacokinetic studies. The results of pharmacokinetic profiling of **31**, **33**, **35**, **36**, and **38** in male Sprague–Dawley rats are described in Table 4. While **35** and **38** displayed less favorable profiles such as moderate to high clearance, **31**, **33**, and **36** exhibited both low clearance and good bioavailability. Clearance was much higher for **35** presumably due in part to oxidative metabolism in the *ortho*-methyl group, although hydroxylation in the *para* position may also play a part as clearance was somewhat improved when a *para*-F was introduced as in compound **38**. Improvement in clearance over **35** is further observed with *ortho*-Cl analogue (**36**), but remained higher than the *ortho*, *para*-di-F analogue (**31**), suggesting *para*-hydroxylation was a site of oxidative metabolism.

In a kinase profiling study to probe potential off-target liabilities, compound **31** exhibited activity against p38 α and p38 β (IC₅₀ = 4.8 nM) and was selective against the other two isoforms, p38 γ and p38 δ (IC₅₀ > 10 μ M).¹⁷ In an Ambit screen,¹⁸ **31** was devoid of activity against over 300 protein kinases with the exception of cKit, PDGFR, and ZAK, where **31** displayed moderate activity (POC < 35% at 1 μ M). In addition, **31** did not show any activity against a variety of G-protein-coupled receptors and ion channels when tested at 10 μ M concentration. In a cardiovascular safety screen, compound **31** displayed an IC₅₀ of 19.5 μ M for blockade of the hERG cardiac channel determined by electrophysiology.

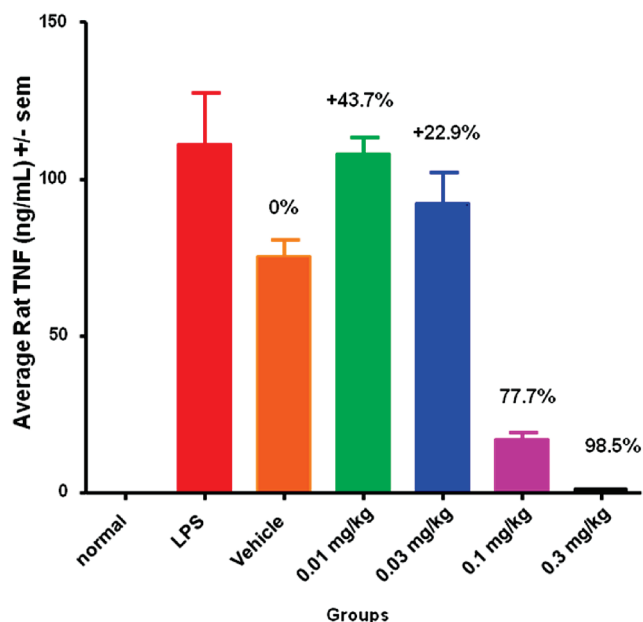


Figure 6. Effect of **31** on LPS-Induced TNF α in Lewis rats.

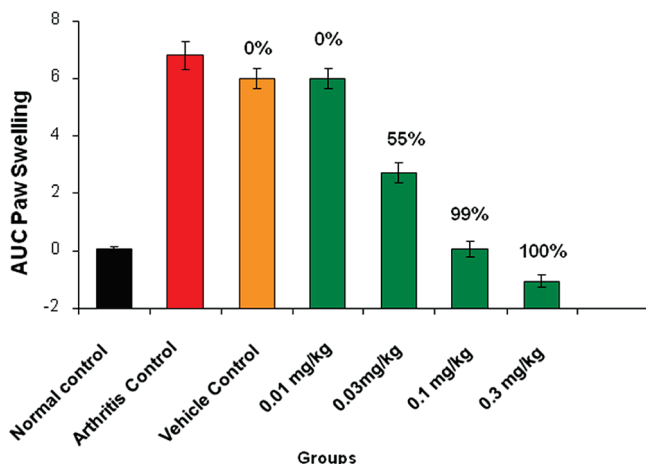


Figure 7. Effect of **31** on paw swelling in Lewis rats in collagen-induced arthritis.

The excellent in vitro selectivity and safety profile demonstrated by **31** warranted further development.

In Vivo Pharmacology. Compound **31** was further evaluated in an acute biochemical challenge model-lipopolysaccharides (LPS) induced TNF α production in female Lewis rats. In these studies, vehicle or compound was given to the rats 1 h prior to injection of LPS, and plasma TNF α levels were determined after 90 min. As illustrated in Figure 6, **31** showed dose-dependent inhibition of TNF α production with an ED₅₀ about 0.06 mg/kg. In a collagen-induced arthritis (CIA) model in Lewis rats, compound **31** showed a dose-dependent reduction in paw swelling with an ED₅₀ of 0.03 mg/kg (Figure 7).

Conclusion

On the basis of the insight provided by X-ray crystallography of potent p38 inhibitors **1** and **2**, we have designed a novel pyridazinopyridinone scaffold by merging the key pharmacophoric elements of the phthalazine and pyrazolopyridinone series. Through focused SAR studies guided by

protein crystallography, several compounds were identified as potent inhibitors in enzyme, cell and whole blood assays. Among them, compound **31** demonstrated favorable pharmacokinetic properties with low clearance and good bioavailability, and also exhibited excellent selectivity against a panel of over 300 kinases. In addition, **31** displayed dose-dependent effects in both acute biochemical challenge and chronic disease models with ED₅₀ values of 0.06 and 0.03 mg/kg, respectively.

Experimental Section

Chemistry. Unless otherwise noted, all materials were obtained from commercial suppliers and used without further purification. Anhydrous solvents were obtained from Aldrich or EM Science and used directly. All reactions involving air- or moisture-sensitive reagents were performed under a nitrogen or argon atmosphere. All microwave-assisted reactions were conducted with an Initiator microwave reactor from Personal Chemistry, Biotage AB, Uppsala, Sweden. All final compounds were purified to >95% purity as determined by LC/MS obtained on Agilent 1100 spectrometers using one of the three following methods: HPLC Method A: YMCODS-AM (100 × 2.1 mm, 5 μ m, 40 °C); mobile phase: A = 0.1% HCOOH in water, B = 0.1% HCOOH in acetonitrile; gradient: 0.0–0.5 min, 10% B; 0.5–7.0 min, 10–100% B; 7.0–9.5 min, 100% B; 9.5–10.0 min, 100–10% B; flow rate = 0.5 mL/min; λ = 254 nm; 1.5 min post time; 3.0 μ L injection. HPLC Method B: Phenomenex Synergi MAX-RP (50 × 2.0 mm, 4.0 μ m, 40 °C); mobile phase: A = 0.1% TFA in water, B = 0.1% TFA in acetonitrile; gradient: 0.0–0.2 min, 10% B, 0.2–3.0 min, 10–100% B, 3.0–4.5 min, 100% B, 4.5–5.0 min, 100–10% B; flow rate = 0.8 mL/min; λ = 254 nm; 1.5 min post time; 3.0 μ L injection. HPLC Method C: Agilent SB-C18 column (50 × 3 mm, 3.5 μ m, 40 °C); mobile phase: A = 0.1% TFA in Water, B = 0.1% TFA in acetonitrile; gradient: 0.0–3.0 min, 5–95% B; 3.0–3.5 min, 95% B; 3.5–3.6 min, 95–5% B; flow rate = 1.5 mL/min; λ = 254 nm; 0 min post time; 3.0 μ L injection. Silica gel chromatography was performed using either glass columns packed with silica gel (200–400 mesh, Aldrich Chemical) or prepacked silica gel cartridges (Biotage or RediSep). ¹H NMR spectra were determined with a DRX 400 MHz spectrometer. Chemical shifts are reported in parts per million (ppm, δ units). Low-resolution mass spectral (MS) data were determined on an Agilent 1100 spectrometer using ES ionization modes (positive or negative). High-resolution mass spectral (HRMS) data were determined on an Agilent LC/MSD TOF 1200 series spectrometer. Combustion analyses were performed by Atlantic Micro-lab, Inc., Norcross, GA, and were within $\pm 0.4\%$ of calculated values unless otherwise noted.

2-(4-Methoxybenzyl)-4,5-dibromopyridazin-3(2H)-one (6). A mixture of 4,5-dibromopyridazin-3(2H)-one (**5**) (10.0 g, 39.4 mmol), 4-methoxybenzyl chloride (5.61 mL, 41.4 mmol), tetrabutylammonium bromide (0.635 g, 1.97 mmol), and potassium carbonate (13.6 g, 98.5 mmol) in acetonitrile (80 mL) was heated at 60 °C for 12 h. The mixture was cooled to room temperature and then filtered through a plug of Celite. The filtrate was concentrated to dryness and then sonicated in MeOH. The solid was collected by filtration and washed with MeOH. The solid was dried in vacuo to afford **6** (8.81 g, 60% yield) as a light brown solid. ¹H NMR (400 MHz, CDCl₃) δ ppm 7.78 (1 H, s), 7.40 (2 H, d, *J* = 8.6 Hz), 6.85 (2 H, d, *J* = 8.8 Hz), 5.25 (2 H, s), 3.78 (3 H, s); MS (ESI, pos. ion) *m/z*: 375 (M + 1).

2-(4-Methoxybenzyl)-5-bromo-4-(methylamino)pyridazin-3(2H)-one (7) and 2-(4-Methoxybenzyl)-4-bromo-5-(methylamino)pyridazin-3(2H)-one (8). **Method A.** To a microwave vial containing 2-(4-methoxybenzyl)-4,5-dibromopyridazin-3(2H)-one **6** (0.475 g, 1.27 mmol) was added *p*-dioxane (5 mL) saturated with MeNH₂. The reaction vessel was sealed and heated in a microwave at 100 °C for 1 h, then cooled to room temperature. The solvent was then

removed in vacuo and the residue was purified by silica gel column chromatography (10–40% EtOAc in hexanes) to give **7** (0.258 g, 62.7% yield) as a white solid and **8** (0.124 g, 30.1% yield) as a white solid. **7**: ^1H NMR (400 MHz, CDCl_3) δ ppm 7.59 (1 H, s), 7.35 (2 H, d, $J = 8.6$ Hz), 6.84 (2 H, d, $J = 8.8$ Hz), 5.95 (1 H, br. s.), 5.17 (2 H, s), 3.78 (3 H, s), 3.30 (3 H, d, $J = 5.7$ Hz); MS (ESI, pos. ion) m/z : 324 ($M + 1$). **8**: ^1H NMR (400 MHz, CDCl_3) δ ppm 7.49 (1 H, s), 7.39 (2 H, d, $J = 8.6$ Hz), 6.84 (2 H, d, $J = 8.6$ Hz), 5.25 (2 H, s), 4.75 (1 H, br. s.), 3.77 (3 H, s), 3.03 (3 H, d, $J = 5.1$ Hz); MS (ESI, pos. ion) m/z : 324 ($M + 1$).

Method B. To a sealed tube was added **6** (18.0 g, 48.1 mmol) in toluene (250 mL, saturated with MeNH_2). The reaction was heated in an oil bath at 90 °C for 18 h, and then the solvent was removed in vacuo. The residue was purified by silica gel column chromatography (10–40% EtOAc in hexanes) to give **7** (12.6 g, 80.8% yield) as a white solid.

1-(4-Methoxybenzyl)-5-(methylamino)-6-oxo-1,6-dihydropyridazine-4-carbonitrile (9). To a microwave vial containing a suspension of **7** (2.24 g, 6.91 mmol) in DMF (12 mL) was added copper cyanide (0.743 g, 8.29 mmol). The reaction was heated in a microwave at 200 °C for 1 h. The reaction mixture was then diluted with a solution of FeCl_3 (10.0 g), conc. HCl (3.0 mL) and water (50 mL) and heated in an oil bath at 70 °C for 15 min, then cooled to room temperature. The mixture was filtered and the solid was washed with water to give **9** (1.75 g, 93.7% yield) as a pale yellow solid. ^1H NMR (400 MHz, CDCl_3) δ ppm 7.56 (1 H, s), 7.35 (2 H, d, $J = 8.6$ Hz), 6.85 (2 H, d, $J = 8.6$ Hz), 5.16 (2 H, s), 3.78 (3 H, s), 3.37 (3 H, d, $J = 5.9$ Hz); MS (ESI, pos. ion) m/z : 271 ($M + 1$).

1-(4-Methoxybenzyl)-*N*-methoxy-*N*-methyl-5-(methylamino)-6-oxo-1,6-dihydropyridazine-4-carboxamide (11). A glass pressure vessel equipped with CO regulator was charged with **7** (7.00 g, 21.5 mmol), *n*,*o*-dimethylhydroxylamine hydrochloride (3.20 g, 32.8 mmol), potassium phosphate (14 g, 65 mmol), and toluene (60 mL). The mixture was purged with Ar then palladium (ii) acetate (0.24 g, 1.1 mmol) and XantPhos (1.20 g, 2.2 mmol) were added. The vessel was sealed and charged with CO (30 psi) and the reaction mixture was stirred in a 110 °C oil bath behind a blast shield for 44 h. After being cooled to room temperature, the reaction mixture was partitioned between water and DCM. The whole mixture was filtered through a pad of Celite and washed with DCM. The organic layer was separated, dried (Na_2SO_4), filtered, and concentrated in vacuo. The residue was purified by silica gel column chromatography (0–3% MeOH in DCM) to give **11** (4.60 g, 64.2% yield) as a yellow foam. ^1H NMR (400 MHz, $\text{DMSO}-d_6$) δ ppm 7.52 (1 H, s), 7.19–7.31 (3 H, m), 6.81–6.94 (2 H, m), 5.12 (2 H, s), 3.72 (3 H, s), 3.57 (3 H, s), 3.23 (3 H, s), 2.70 (3 H, d, $J = 5.5$ Hz); MS (ESI, pos. ion) m/z : 333 ($M + 1$).

1-(4-Methoxybenzyl)-5-(methylamino)-6-oxo-1,6-dihydropyridazine-4-carbaldehyde (10). **Method A.** To a suspension of **9** (5.50 g, 20.3 mmol) in toluene at 0 °C was added diisobutylaluminum hydride (44.8 mL, 44.8 mmol, 1 M solution in hexanes) dropwise. The reaction was stirred at 0 °C for 20 min, then EtOAc (50 mL) was added and the mixture was warmed to room temperature. After 20 min, 1 M HCl (120 mL) was added and the mixture was heated at 50 °C for 4 h, then filtered through a plug of Celite and washed with EtOAc. The aqueous layer was extracted with EtOAc and the combined organic layers were dried (MgSO_4), filtered, and concentrated in vacuo. The residue was purified by silica gel column chromatography (20–35% EtOAc in hexanes) to give **10** (3.27 g, 58.8% yield) as a light yellow solid. ^1H NMR (400 MHz, CDCl_3) δ ppm 9.52–10.19 (1 H, m), 7.72 (1 H, br. s.), 7.38 (2 H, d, $J = 8.6$ Hz), 6.80–6.96 (2 H, m), 5.15 (2 H, s), 3.78 (3 H, s), 3.57 (3 H, br. s.); MS (ESI, pos. ion) m/z : 274 ($M + 1$).

Method B. To a solution of **11** (4.60 g, 13.8 mmol) in THF (50.0 mL) was added lithium aluminum hydride (1 M solution in THF) (15.23 mL, 15.23 mmol) at –78 °C. The mixture was then stirred at 0 °C for 1 h. The reaction mixture was quenched at 0 °C

very slowly with MeOH (1.0 mL), water (1.0 mL) and 1 M HCl aqueous solution (1.0 mL). The reaction mixture was then filtered off and the filtrate was concentrated to give **10** (3.82 g, 100% yield), which was subjected to the next step without purification.

Ethyl 7-(4-methoxybenzyl)-1-methyl-2,8-dioxo-1,2,7,8-tetrahydropyrido[2,3-*d*]pyridazine-3-carboxylate (13). A mixture of **10** (3.78 g, 13.8 mmol), diethyl malonate (**12**) (4.20 mL, 27.7 mmol), piperidine (1.44 mL, 14.5 mmol), and EtOH (100 mL) was stirred at reflux in an oil bath for 5 h. The reaction mixture was allowed to stand at room temperature overnight to afford a suspension. The solid was collected by suction filtration, washed with EtOH (10 mL), and dried in vacuo to afford **13** (3.27 g, 63.9% yield) as a tan solid. ^1H NMR (400 MHz, $\text{DMSO}-d_6$) δ ppm 8.38 (s, 1 H), 8.27 (s, 1 H), 7.31 (2 H, d, $J = 8.6$ Hz), 6.89 (2 H, d, $J = 8.6$ Hz), 5.21 (s, 2 H), 4.29 (2 H, q, $J = 7.1$ Hz), 4.01 (s, 3 H), 3.72 (s, 3 H), 1.29 (3 H, t, $J = 7.0$ Hz); MS (ESI, pos. ion) m/z : 370 ($M + 1$).

Ethyl 8-Chloro-1-methyl-2-oxo-1,2-dihydropyrido[3,2-*d*]pyridazine-3-carboxylate (14). A microwave vial was charged with **13** (2.00 g, 5.41 mmol) in TFA (12 mL). The reaction was heated in a microwave at 125 °C for 2 h, cooled to room temperature, and then the solvent was removed in vacuo. The residue was diluted with DCM (100 mL) and concentrated in vacuo. The crude product was dissolved in phosphorus oxychloride (8.00 mL, 85.8 mmol), and the solution was heated to reflux at 110 °C for 1 h in an oil bath. The mixture was cooled to room temperature. The solvent was removed in vacuo, and the residue was triturated with DCM. The suspension was filtered to give **14** (1.25 g, 86.2% yield) as a light green solid. ^1H NMR (400 MHz, CDCl_3) δ ppm 9.11 (1 H, s), 8.29 (1 H, s), 4.45 (2 H, q, $J = 7.0$ Hz), 4.09 (3 H, s), 1.43 (3 H, t, $J = 7.1$ Hz); MS (ESI, pos. ion) m/z : 268 ($M + 1$).

8-(2,4-Difluorophenyl)-1-methyl-2-oxo-1,2-dihydropyrido[3,2-*d*]pyridazine-3-carboxylic acid (15). A microwave vial was charged with **14** (0.75 g, 2.80 mmol), 2,4-difluorobenzeneboronic acid (0.53 g, 3.36 mmol), and tetrakis(triphenylphosphine)-palladium (0.26 g, 0.23 mmol) in *p*-dioxane/2 M aq. Na_2CO_3 (4:1, 12.5 mL). The reaction was heated in a microwave at 105 °C for 90 min, and then 1 M aq. NaOH (1.5 mL) was added. The reaction was heated in a microwave at 105 °C for 1 h, and then cooled to room temperature. The reaction was repeated once on a 0.75 g scale. The two reaction mixtures were combined and extracted with DCM. The aqueous layer was acidified with conc. HCl to pH ~ 2 and extracted with $\text{CHCl}_3/\text{iPrOH}$ (4:1). The combined organic layers were dried (MgSO_4), filtered, and concentrated in vacuo to give **15** (1.28 g, 72.0% yield) as an orange solid. ^1H NMR (400 MHz, $\text{DMSO}-d_6$) δ ppm 9.57 (1 H, s), 8.77 (1 H, s), 7.76–7.91 (1 H, m), 7.44–7.59 (1 H, m), 7.26–7.44 (1 H, m), 3.13 (3 H, s); MS (ESI, pos. ion) m/z : 318 ($M + 1$).

3-Bromo-8-(2,4-difluorophenyl)-1-methylpyrido[3,2-*d*]pyridazin-2(1H)-one (16). To a suspension of **15** (4.51 g, 14.2 mmol) in THF/ H_2O (10:1, 55 mL) was added lithium acetate dihydrate (0.218 g, 2.13 mmol) followed by *n*-bromosuccinimide (3.16 g, 17.8 mmol). The reaction was heated at 55 °C in an oil bath for 30 min, and then another 1.25 eq of *n*-bromosuccinimide was added. The reaction was stirred an additional 30 min before being cooled to room temperature. The mixture was diluted with water and extracted with DCM. The combined organic layers were dried (MgSO_4), filtered, and concentrated in vacuo. The residue was purified by silica gel column chromatography (5–15% EtOAc in DCM with 1% MeOH) to give **16** (4.05 g, 80.9% yield) as a light yellow solid. ^1H NMR (400 MHz, CDCl_3) δ ppm 9.17 (1 H, s), 8.25 (1 H, s), 7.72–7.85 (1 H, m), 7.09–7.20 (1 H, m), 6.92–7.05 (1 H, m), 3.36 (3 H, s); MS (ESI, pos. ion) m/z : 352 ($M + 1$).

8-(2,4-Difluorophenyl)-3-(4-fluorophenylamino)-1-methylpyrido[3,2-*d*]pyridazin-2(1H)-one (17). A microwave vial was charged with **16** (0.10 g, 0.284 mmol) in toluene (1 mL), 4-fluoroaniline (0.034 mL, 0.355 mmol), palladium acetate (3.19 mg, 0.014 mmol),

cesium carbonate (0.139 g, 0.426 mmol), and 4,5-bis(diphenylphosphino)-9,9-dimethylxanthene (0.016 mg, 0.028 mmol). The reaction was heated in a microwave at 125 °C for 30 min. The mixture was diluted with water, and filtered, and the resulting solid was washed with water, toluene, then dried to give **17** (0.078 g, 71.8% yield) as a yellow solid. ¹H NMR (400 MHz, DMSO-*d*₆) δ ppm 9.26 (1 H, s), 8.85 (1 H, s), 7.74–7.86 (1 H, m), 7.42–7.55 (3 H, m), 7.21–7.38 (4 H, m), 3.21 (3 H, s); HRMS(TOF-MS) calcd: 383.1114 for C₂₀H₁₄F₃N₄O [M + H]⁺. Found: 383.1111; HPLC (Method A); retention time 6.45 min.

8-(2,4-Difluorophenyl)-3-(2,4-difluorophenylamino)-1-methylpyrido[3,2-*d*]pyridazin-2(1H)-one (18). The title compound (30 mg, 26%) was prepared according to the procedure described for compound **17** from **16** (100 mg, 0.284 mmol) and 2,4-difluorobenzeneamine (45.8 mg, 0.355 mmol). **18**: ¹H NMR (400 MHz, DMSO-*d*₆) δ ppm 9.25 (1 H, s), 8.64 (1 H, s), 7.72–7.88 (1 H, m), 7.41–7.61 (3 H, m), 7.32 (1 H, td, *J* = 8.5, 1.9 Hz), 7.21 (1 H, t, *J* = 9.4 Hz), 6.76 (1 H, d, *J* = 2.3 Hz), 3.21 (3 H, s); HRMS(TOF-MS) calcd: 401.1020 for C₂₀H₁₃F₄N₄O [M + H]⁺. Found: 401.1022; HPLC (method A); retention time 6.24 min.

8-(2,4-Difluorophenyl)-3-(5-fluoropyridin-2-ylamino)-1-methylpyrido[3,2-*d*]pyridazin-2(1H)-one (19). The title compound (31 mg, 48%) was prepared according to the procedure described for compound **17** from **16** (60 mg, 0.17 mmol) and 2-amino-5-fluoropyridine (23 mg, 0.21 mmol). **19**: ¹H NMR (400 MHz, DMSO-*d*₆) δ ppm 9.59 (1 H, s), 9.38 (1 H, s), 8.88 (1 H, s), 8.37 (1 H, d, *J* = 2.9 Hz), 7.68–7.87 (2 H, m), 7.60 (1 H, dd, *J* = 9.3, 3.8 Hz), 7.41–7.53 (1 H, m), 7.28–7.39 (1 H, m), 3.22 (3 H, s); HRMS(TOF-MS) calcd: 384.1067 for C₁₉H₁₃F₃N₅O [M + H]⁺. Found: 384.1064; HPLC (Method B); retention time 1.86 min.

8-(2,4-Difluorophenyl)-3-(3,5-difluoropyridin-2-ylamino)-1-methylpyrido[3,2-*d*]pyridazin-2(1H)-one (20). The title compound (27 mg, 47%) was prepared according to the procedure described for compound **17** from **16** (50 mg, 0.14 mmol) and 3,5-difluoropyridin-2-amine (28 mg, 0.21 mmol). **20**: ¹H NMR (400 MHz, CDCl₃) δ ppm 9.29 (1 H, s), 8.90 (1 H, s), 8.57 (1 H, br. s.), 8.18 (1 H, d, *J* = 2.5 Hz), 7.78 (1 H, td, *J* = 8.4, 6.3 Hz), 7.32 (1 H, ddd, *J* = 10.0, 7.6, 2.5 Hz), 7.14 (1 H, td, *J* = 8.2, 2.2 Hz), 6.92–7.04 (1 H, m), 3.42 (3 H, s); HRMS(TOF-MS) calcd: 402.0973 for C₁₉H₁₂F₄N₅O [M + H]⁺. Found: 402.0971; HPLC (Method B); retention time 2.38 min.

8-(2,4-Difluorophenyl)-3-((4-fluorophenyl)(methyl)amino)-1-methylpyrido[3,2-*d*]pyridazin-2(1H)-one (21). The title compound (22 mg, 40%) was prepared according to the procedure described for compound **17** from **16** (50 mg, 0.14 mmol) and 4-fluoro-*N*-methylaniline (21 mg, 0.17 mmol). **21**: ¹H NMR (400 MHz, DMSO-*d*₆) δ ppm 9.36 (1 H, s), 7.72–7.84 (1 H, m), 7.51 (1 H, s), 7.41–7.50 (1 H, m), 7.28–7.36 (1 H, m), 7.05–7.15 (4 H, m), 3.35 (3 H, s), 3.02 (3 H, s); HRMS(TOF-MS) calcd: 397.1271 for C₂₁H₁₆F₃N₄O [M + H]⁺. Found: 397.1269; HPLC (Method B); retention time 1.87 min.

8-(2,4-Difluorophenyl)-3-(4-fluorophenoxy)-1-methylpyrido[3,2-*d*]pyridazin-2(1H)-one (22). The title compound (23 mg, 36%) was prepared according to the procedure described for compound **17** from **16** (60 mg, 0.14 mmol) and 4-fluorophenol (29 mg, 0.26 mmol). **22**: ¹H NMR (400 MHz, DMSO-*d*₆) δ ppm 9.36 (1 H, s), 7.79 (1 H, q, *J* = 7.8 Hz), 7.48 (1 H, t, *J* = 9.1 Hz), 7.23–7.41 (6 H, m), 3.16 (3 H, s); HRMS(TOF-MS) calcd: 384.0954 for C₂₀H₁₃F₃N₃O₂ [M + H]⁺. Found: 384.0953; HPLC (Method A); retention time 6.05 min.

3-(2,4-Difluorophenoxy)-8-(2,4-difluorophenyl)-1-methylpyrido[3,2-*d*]pyridazin-2(1H)-one (23). The title compound (18 mg, 32%) was prepared according to the procedure described for compound **17** from **16** (50 mg, 0.14 mmol) and 2,4-difluorophenol (23 mg, 0.18 mmol). **23**: ¹H NMR (400 MHz, DMSO-*d*₆) δ ppm 9.36 (1 H, s), 7.79 (1 H, td, *J* = 8.6, 6.6 Hz), 7.61 (1 H, ddd, *J* = 11.2, 8.7, 3.0 Hz), 7.45–7.56 (2 H, m), 7.41 (1 H, s), 7.34 (1 H, td, *J* = 8.4, 2.0 Hz), 7.21–7.29 (1 H, m), 3.16 (3 H, s); HRMS(TOF-MS) calcd: 402.0860 for C₂₀H₁₂F₄N₃O₂ [M + H]⁺. Found: 402.0858; HPLC (Method A); retention time 6.25 min.

3-(4-Fluorobenzyl)-8-(2,4-difluorophenyl)-1-methylpyrido[3,2-*d*]pyridazin-2(1H)-one (24). A microwave vial was charged with **16** (0.050 g, 0.14 mmol) in THF (0.5 mL), tetrakis(triphenylphosphine)palladium (0.010 g, 0.0091 mmol), and 4-fluorobenzylzinc chloride (0.5 M solution in THF) (0.5 mL, 0.25 mmol). The reaction was heated in an oil bath at 75 °C for 1 h, and then cooled to room temperature. The reaction was quenched with sat. NH₄Cl and the mixture was extracted with EtOAc. The combined organic layers were dried (MgSO₄), filtered, and concentrated in vacuo. The residue was purified by silica gel column chromatography (35–85% EtOAc in hexanes) to give **24** (16 mg, 30% yield). ¹H NMR (400 MHz, DMSO-*d*₆) δ ppm 9.37 (1 H, s), 7.87 (1 H, s), 7.79 (1 H, td, *J* = 8.5, 6.7 Hz), 7.42–7.51 (1 H, m), 7.28–7.42 (3 H, m), 7.16 (2 H, t, *J* = 8.9 Hz), 3.94 (2 H, s), 3.10 (3 H, s); HRMS(TOF-MS) calcd: 382.1162 for C₂₁H₁₅F₃N₃O [M + H]⁺. Found: 382.1168; HPLC (Method C); retention time 2.05 min.

3-(2,4-Difluorobenzyl)-8-(2,4-difluorophenyl)-1-methylpyrido[3,2-*d*]pyridazin-2(1H)-one (25). The title compound (34 mg, 60%) was prepared according to the procedure described for compound **24** from **16** (50 mg, 0.14 mmol) and (2,4-difluorobenzyl)zinc(II) bromide (0.4 mL, 0.5 M). **25**: ¹H NMR (400 MHz, DMSO-*d*₆) δ ppm 9.40 (1 H, s), 7.74–7.86 (2 H, m), 7.39–7.52 (2 H, m), 7.22–7.38 (2 H, m), 7.09 (1 H, td, *J* = 8.6, 1.9 Hz), 3.95 (2 H, s), 3.11 (3 H, s); HRMS(TOF-MS) calcd: 400.1068 for C₂₁H₁₄F₄N₃O [M + H]⁺. Found: 400.1074; HPLC (Method C); retention time 2.10 min.

3-(8-(2,4-Difluorophenyl)-1-methyl-2-oxo-1,2-dihydropyrido[3,2-*d*]pyridazin-3-yl)-4-methylbenzoic acid (26). To a sealed vessel was added **16** (2.00 g, 5.68 mmol) in *p*-dioxane/H₂O (4:1, 50 mL), 3-borono-4-methylbenzoic acid (1.124 g, 6.25 mmol), sodium carbonate monohydrate (1.761 g, 14.20 mmol), and tetrakis(triphenylphosphine) palladium (0.328 g, 0.284 mmol). The reaction was heated in oil bath at 105 °C for 8 h, and then at 55 °C overnight. The reaction mixture was diluted with 1 N NaOH and washed with DCM twice. The aqueous layer was acidified with 5 N HCl to pH 2, and the resulting suspension was filtered to give **26** (1.98 g, 85.4% yield) as an off-white solid. ¹H NMR (400 MHz, DMSO-*d*₆) δ ppm 9.45 (1 H, s), 8.21 (1 H, s), 7.92 (1 H, dd, *J* = 7.8, 1.8 Hz), 7.80–7.89 (2 H, m), 7.43–7.55 (2 H, m), 7.36 (1 H, td, *J* = 8.6, 2.4 Hz), 3.15 (3 H, s), 2.25 (3 H, s); MS (ESI, pos. ion) *m/z*: 408 (M + 1); HPLC (Method B); retention time 1.71 min.

4-Chloro-3-(8-(2,4-difluorophenyl)-1-methyl-2-oxo-1,2-dihydropyrido[3,2-*d*]pyridazin-3-yl)benzoic acid (27). The title compound (15 mg, 10%) was prepared according to the procedure described for compound **26** from **16** (120 mg, 0.34 mmol) and 4-chloro-3-(4,4,5,5-tetramethyl-1,3,2-dioxaborolan-2-yl)benzoic acid (116 mg, 0.41 mmol). **27**: ¹H NMR (400 MHz, DMSO-*d*₆) δ ppm 13.32 (1 H, br. s.), 9.46 (1 H, s), 8.32 (1 H, s), 7.98–8.05 (2 H, m), 7.87 (1 H, td, *J* = 8.6, 6.7 Hz), 7.70–7.78 (1 H, m), 7.50 (1 H, td, *J* = 9.7, 2.4 Hz), 7.37 (1 H, td, *J* = 8.5, 2.2 Hz), 3.16 (3 H, s); MS (ESI, pos. ion) *m/z*: 428 (M + 1).

3-(8-(2,4-Difluorophenyl)-1-methyl-2-oxo-1,2-dihydropyrido[3,2-*d*]pyridazin-3-yl)-*N*,4-dimethylbenzamide (28). To a solution of **26** (0.100 g, 0.245 mmol) in DMSO (1.5 mL) was added triethylamine (85 μL, 0.614 mmol), 2-(1H-7-azabenzotriazol-1-yl)-1,1,3,3-tetramethyl uronium hexafluorophosphate methanaminium (0.140 g, 0.368 mmol), followed by MeNH₂ in THF (2 M, 0.6 mL, 1.2 mmol). The reaction was stirred at room temperature for 30 min, and then was diluted with CHCl₃/iPrOH (4:1). The mixture was washed with water four times, dried (MgSO₄), filtered, and concentrated in vacuo. The residue was purified by silica gel column chromatography (40–50% EtOAc in DCM with 1% MeOH) to give **28** (64.0 mg, 62.0% yield) as a white solid. ¹H NMR (400 MHz, DMSO-*d*₆) δ ppm 9.45 (1 H, s), 8.37–8.47 (1 H, m), 8.19 (1 H, s), 7.79–7.92 (2 H, m), 7.76 (1 H, s), 7.45–7.55 (1 H, m), 7.31–7.44 (2 H, m), 3.16 (3 H, s), 2.78 (3 H, d, *J* = 4.3 Hz), 2.21 (3 H, s); HRMS(TOF-MS) calcd: 421.1471 for C₂₃H₁₉F₂N₄O₂ [M + H]⁺. Found: 421.1473; HPLC (Method A); retention time 5.43 min.

4-Chloro-*N*-cyclopropyl-3-(8-(2,4-difluorophenyl)-1-methyl-2-oxo-1,2-dihydropyrido[3,2-*d*]pyridazin-3-yl)benzamide (29). The title compound (15 mg, 9%) was prepared according to the procedure described for compound **28** from **27** (150 mg, 0.35 mmol) and cyclopropylamine (100 mg, 1.75 mmol). **29**: ^1H NMR (400 MHz, DMSO- d_6) δ ppm 9.46 (1 H, s), 8.56 (1 H, d, $J = 3.7$ Hz), 8.29 (1 H, s), 7.82–7.97 (3 H, m), 7.69 (1 H, d, $J = 9.2$ Hz), 7.43–7.57 (1 H, m), 7.37 (1 H, td, $J = 8.9, 2.7$ Hz), 3.16 (3 H, s), 2.81–2.92 (1 H, m), 0.66–0.75 (2 H, m), 0.54–0.61 (2 H, m); HRMS(ToF-MS) calcd: 467.1081 for $\text{C}_{24}\text{H}_{18}\text{ClF}_2\text{N}_4\text{O}_2$ [$\text{M} + \text{H}$] $^+$. Found: 467.1085; HPLC (Method A); retention time 5.88 min.

3-(8-(2,4-Difluorophenyl)-1-methyl-2-oxo-1,2-dihydropyrido[3,2-*d*]pyridazin-3-yl)-4-methylbenzamide (30). A microwave vial was charged with **16** (0.022 g, 0.062 mmol) in *p*-dioxane/1 M Na_2CO_3 (3:1, 1.6 mL), 4-methyl-3-(4,4,5,5-tetramethyl-1,3,2-dioxaborolan-2-yl)benzamide (0.018 mg, 0.069 mmol) 16d and tetrakis(triphenylphosphine) palladium (0.0058 g, 0.005 mmol). The reaction was heated in a microwave at 100 °C for 50 min. The mixture was diluted with water and extracted with $\text{CHCl}_3/\text{iPrOH}$ (4:1). The combined organic layers were dried (MgSO_4), filtered, and concentrated in vacuo. The residue was purified with reverse phase HPLC to give **30** (0.008 g, 32% yield) as a white solid. ^1H NMR (400 MHz, DMSO- d_6) δ ppm 9.45 (1 H, s), 8.20 (1 H, s), 7.96 (1 H, br. s.), 7.83–7.91 (2 H, m), 7.81 (1 H, d, $J = 1.6$ Hz), 7.46–7.55 (1 H, m), 7.29–7.44 (3 H, m), 3.16 (3 H, s), 2.22 (3 H, s); HRMS(ToF-MS) calcd: 407.1314 for $\text{C}_{22}\text{H}_{17}\text{F}_2\text{N}_4\text{O}_2$ [$\text{M} + \text{H}$] $^+$. Found: 407.1317; HPLC (Method B); retention time 1.56 min.

***N*-Cyclopropyl-3-(8-(2,4-difluorophenyl)-1-methyl-2-oxo-1,2-dihydropyrido[3,2-*d*]pyridazin-3-yl)-4-methylbenzamide (31).** The title compound (1.89 g, 60%) was prepared according to the procedure described for compound **30** from **16** (2.5 g, 7.10 mmol) and *N*-cyclopropyl-4-methyl-3-(4,4,5,5-tetramethyl-1,3,2-dioxaborolan-2-yl)benzamide (2.46 g, 8.17 mmol). **31**: ^1H NMR (400 MHz, DMSO- d_6) δ ppm 9.45 (1 H, s), 8.40 (1 H, d, $J = 3.9$ Hz), 8.19 (1 H, s), 7.78–7.92 (2 H, m), 7.74 (1 H, s), 7.50 (1 H, td, $J = 9.6, 2.2$ Hz), 7.32–7.42 (2 H, m), 3.16 (3 H, s), 2.80–2.90 (1 H, m), 2.21 (3 H, s), 0.64–0.74 (2 H, m), 0.52–0.61 (2 H, m); HRMS(ToF-MS) calcd: 447.1627 for $\text{C}_{25}\text{H}_{21}\text{F}_2\text{N}_4\text{O}_2$ [$\text{M} + \text{H}$] $^+$. Found: 447.1619. Anal. Calcd. for $\text{C}_{25}\text{H}_{20}\text{F}_2\text{N}_4\text{O}_2$: C, 67.26; H, 4.52; N, 12.55; F, 8.51. Found: C, 67.09; H, 4.48; N, 12.33; F, 8.52; HPLC (Method A); retention time 5.71 min.

3-(8-(2,4-Difluorophenyl)-1-methyl-2-oxo-1,2-dihydropyrido[3,2-*d*]pyridazin-3-yl)-4-methyl-*N*-(1-methylcyclopropyl)benzamide (32). The title compound (41 mg, 63%) was prepared according to the procedure described for compound **30** from **16** (50 mg, 0.14 mmol) and 4-methyl-*N*-(1-methylcyclopropyl)-3-(4,4,5,5-tetramethyl-1,3,2-dioxaborolan-2-yl)benzamide (52 mg, 0.16 mmol). 16d **32**: ^1H NMR (400 MHz, DMSO- d_6) δ ppm 9.45 (1 H, s), 8.63 (1 H, s), 8.19 (1 H, s), 7.78–7.93 (2 H, m), 7.74 (1 H, d, $J = 1.8$ Hz), 7.50 (1 H, td, $J = 9.9, 2.4$ Hz), 7.32–7.42 (2 H, m), 3.16 (3 H, s), 2.20 (3 H, s), 1.36 (3 H, s), 0.69–0.77 (2 H, m), 0.56–0.64 (2 H, m); HRMS(ToF-MS) calcd: 461.1784 for $\text{C}_{26}\text{H}_{23}\text{F}_2\text{N}_4\text{O}_2$ [$\text{M} + \text{H}$] $^+$. Found: 461.1779; HPLC (Method B); retention time 1.84 min.

***N*-Cyclopropyl-3-(8-(2,4-difluorophenyl)-1-methyl-2-oxo-1,2-dihydropyrido[3,2-*d*]pyridazin-3-yl)-5-fluoro-4-methylbenzamide (33).** The title compound (57 mg, 72%) was prepared according to the procedure described for compound **30** from **16** (60 mg, 0.17 mmol) and *N*-cyclopropyl-3-fluoro-4-methyl-5-(4,4,5,5-tetramethyl-1,3,2-dioxaborolan-2-yl)benzamide (65 mg, 0.20 mmol). 16c **33**: ^1H NMR (400 MHz, DMSO- d_6) δ ppm 9.46 (1 H, s), 8.50 (1 H, d, $J = 4.1$ Hz), 8.24 (1 H, s), 7.85 (1 H, td, $J = 8.5, 6.7$ Hz), 7.70 (1 H, d, $J = 10.6$ Hz), 7.64 (1 H, s), 7.50 (1 H, td, $J = 9.7, 2.4$ Hz), 7.36 (1 H, td, $J = 8.4, 2.3$ Hz), 3.15 (3 H, s), 2.80–2.91 (1 H, m), 2.10 (3 H, d, $J = 1.8$ Hz), 0.66–0.75 (2 H, m), 0.51–0.61 (2 H, m); HRMS(ToF-MS) calcd: 465.1533 for $\text{C}_{25}\text{H}_{20}\text{F}_3\text{N}_4\text{O}_2$ [$\text{M} + \text{H}$] $^+$. Found: 465.1534; Anal. Calcd. For $\text{C}_{25}\text{H}_{19}\text{F}_3\text{N}_4\text{O}_2$: C, 64.15; H, 4.12; N, 12.06; F, 12.27. Found: C,

64.08; H, 4.06; N, 11.90; F, 12.38; HPLC (Method A); retention time 6.00 min.

***N*-Cyclopropyl-4-(8-(2,4-difluorophenyl)-1-methyl-2-oxo-1,2-dihydropyrido[3,2-*d*]pyridazin-3-yl)-5-methylpicolinamide (34).** The title compound (8 mg, 10%) was prepared according to the procedure described for compound **30** from **16** (60 mg, 0.17 mmol) and 2-(cyclopropylcarbamoyl)-5-methylpyridin-4-ylboronic acid (45 mg, 0.21 mmol). **34**: ^1H NMR (400 MHz, DMSO- d_6) δ ppm 9.46 (1 H, s), 8.74 (1 H, d, $J = 4.9$ Hz), 8.58 (1 H, s), 8.30 (1 H, s), 7.94 (1 H, s), 7.77–7.90 (1 H, m), 7.51 (1 H, td, $J = 9.9, 2.2$ Hz), 7.30–7.42 (1 H, m), 3.15 (3 H, s), 2.86–2.98 (1 H, m), 2.27 (3 H, s), 0.66–0.74 (4 H, m); HRMS(ToF-MS) calcd: 448.1580 for $\text{C}_{24}\text{H}_{20}\text{F}_2\text{N}_5\text{O}_2$ [$\text{M} + \text{H}$] $^+$. Found: 448.1570; HPLC (Method B); retention time 1.79 min.

***N*-Cyclopropyl-4-methyl-3-(1-methyl-2-oxo-8-*o*-tolyl-1,2-dihydropyrido[3,2-*d*]pyridazin-3-yl)benzamide (35).** The title compound (43.5 mg, 23%) was prepared according to the procedure described for compound **30** from **14** and *o*-tolylboronic acid. **35**: ^1H NMR (400 MHz, DMSO- d_6) δ ppm 9.42 (1 H, s), 8.41 (1 H, d, $J = 3.5$ Hz), 8.17 (1 H, s), 7.81 (1 H, d, $J = 7.0$ Hz), 7.74 (1 H, s), 7.29–7.54 (5 H, m), 3.00 (3 H, s), 2.76–2.92 (1 H, m), 2.21 (3 H, s), 2.12 (3 H, s), 0.64–0.74 (2 H, m), 0.50–0.60 (2 H, m); HRMS(ToF-MS) calcd: 425.1972 for $\text{C}_{26}\text{H}_{25}\text{N}_4\text{O}_2$ [$\text{M} + \text{H}$] $^+$. Found: 425.1968; HPLC (Method A); retention time 5.67 min.

3-(8-(2-Chlorophenyl)-1-methyl-2-oxo-1,2-dihydropyrido[3,2-*d*]pyridazin-3-yl)-*N*-cyclopropyl-4-methylbenzamide (36). The title compound (31 mg, 15%) was prepared according to the procedure described for compound **30** from **14** and 2-chlorophenylboronic acid. **36**: ^1H NMR (400 MHz, DMSO- d_6) δ ppm 9.46 (1 H, s), 8.41 (1 H, d, $J = 3.9$ Hz), 8.20 (1 H, s), 7.77–7.84 (2 H, m), 7.75 (1 H, d, $J = 1.8$ Hz), 7.66–7.70 (1 H, m), 7.56–7.65 (2 H, m), 7.39 (1 H, d, $J = 7.8$ Hz), 3.11 (3 H, s), 2.80–2.89 (1 H, m), 2.20 (3 H, s), 0.65–0.72 (2 H, m), 0.52–0.59 (2 H, m); HRMS(ToF-MS) calcd: 445.1426 for $\text{C}_{25}\text{H}_{22}\text{ClN}_4\text{O}_2$ [$\text{M} + \text{H}$] $^+$. Found: 445.1419; HPLC (Method A); retention time 5.74 min.

***N*-Cyclopropyl-4-methyl-3-(1-methyl-2-oxo-8-(2-(trifluoromethyl)phenyl)-1,2-dihydropyrido[3,2-*d*]pyridazin-3-yl)benzamide (37).** The title compound (31 mg, 14%) was prepared according to the procedure described for compound **30** from **14** and 2-(trifluoromethyl)phenylboronic acid. **37**: ^1H NMR (400 MHz, DMSO- d_6) δ ppm 9.47 (1 H, s), 8.41 (1 H, d, $J = 3.9$ Hz), 8.19 (1 H, s), 7.99 (1 H, d, $J = 7.6$ Hz), 7.78–7.92 (4 H, m), 7.74 (1 H, d, $J = 1.6$ Hz), 7.39 (1 H, d, $J = 8.0$ Hz), 3.03 (3 H, s), 2.80–2.90 (1 H, m), 2.20 (3 H, s), 0.65–0.73 (2 H, m), 0.51–0.61 (2 H, m); HRMS(ToF-MS) calcd: 479.1689 for $\text{C}_{26}\text{H}_{22}\text{F}_3\text{N}_4\text{O}_2$ [$\text{M} + \text{H}$] $^+$. Found: 479.1689; HPLC (Method B); retention time 1.85 min.

***N*-Cyclopropyl-3-(8-(4-fluoro-2-methylphenyl)-1-methyl-2-oxo-1,2-dihydropyrido[3,2-*d*]pyridazin-3-yl)-4-methylbenzamide (38).** The title compound (53 mg, 43%) was prepared according to the procedure described for compound **30** from **14** and 4-fluoro-2-methylphenylboronic acid. **38**: ^1H NMR (400 MHz, DMSO- d_6) δ ppm 9.42 (1 H, s), 8.41 (1 H, d, $J = 4.1$ Hz), 8.17 (1 H, s), 7.81 (1 H, dd, $J = 8.0, 1.8$ Hz), 7.73 (1 H, d, $J = 1.6$ Hz), 7.49 (1 H, dd, $J = 8.5, 6.0$ Hz), 7.38 (1 H, d, $J = 8.0$ Hz), 7.30 (1 H, dd, $J = 9.9, 2.4$ Hz), 7.22 (1 H, td, $J = 8.5, 2.6$ Hz), 3.02 (3 H, s), 2.79–2.90 (1 H, m), 2.21 (3 H, s), 2.14 (3 H, s), 0.64–0.73 (2 H, m), 0.50–0.61 (2 H, m); HRMS(ToF-MS) calcd: 443.1878 for $\text{C}_{26}\text{H}_{24}\text{FN}_4\text{O}_2$ [$\text{M} + \text{H}$] $^+$. Found: 443.1871; HPLC (Method B); retention time 1.75 min.

***N*-Cyclopropyl-3-(8-(2-fluoro-4-(trifluoromethyl)phenyl)-1-methyl-2-oxo-1,2-dihydropyrido[3,2-*d*]pyridazin-3-yl)-4-methylbenzamide (39).** The title compound (35 mg, 14%) was prepared according to the procedure described for compound **30** from **14** and 2-fluoro-4-(trifluoromethyl)phenylboronic acid. **39**: ^1H NMR (400 MHz, DMSO- d_6) δ ppm 9.49 (1 H, s), 8.42 (1 H, d, $J = 4.1$ Hz), 8.21 (1 H, s), 8.07 (1 H, t, $J = 7.5$ Hz), 7.95 (1 H, d, $J = 9.6$ Hz), 7.77–7.91 (2 H, m), 7.75 (1 H, d, $J = 1.6$ Hz), 7.39 (1 H, d, $J = 8.0$ Hz), 3.15 (3 H, s), 2.80–2.90 (1 H, m), 2.21 (3 H, s), 0.63–0.75 (2 H, m), 0.50–0.61 (2 H, m); HRMS(ToF-MS)

calcd: 497.1595 for $C_{26}H_{21}F_4N_4O_2 [M + H]^+$. Found: 497.1594; HPLC (Method A); retention time 6.15 min.

3-(8-(2-Chloro-5-fluorophenyl)-1-methyl-2-oxo-1,2-dihydro-pyrido[2,3-d]pyridazin-3-yl)-N-cyclopropyl-4-methylbenzamide (40). The title compound (396 mg, 23%) was prepared according to the procedure described for compound **30** from **14** and 2-chloro-5-fluorophenylboronic acid. **40**: 1H NMR (400 MHz, DMSO- d_6) δ ppm 9.48 (1 H, s), 8.41 (1 H, d, $J = 3.9$ Hz), 8.20 (1 H, s), 7.82 (1 H, dd, $J = 7.9, 1.7$ Hz), 7.69–7.77 (3 H, m), 7.47–7.59 (1 H, m), 7.39 (1 H, d, $J = 8.0$ Hz), 3.15 (3 H, s), 2.80–2.90 (1 H, m), 2.20 (3 H, s), 0.65–0.73 (2 H, m), 0.53–0.59 (2 H, m); HRMS (TOF-MS) calcd: 463.1332 for $C_{25}H_{21}ClF_4N_4O_2 [M + H]^+$. Found: 463.1333; HPLC (Method B); retention time 1.91 min.

Biological Methods. p38 α MAP Kinase in Vitro Assay. The p38 α kinase reaction was carried out in a polypropylene 96-well black round bottomed assay plate in a total volume of 30 μ L of kinase reaction buffer (50 mM Tris-pH 7.5, 5 mM $MgCl_2$, 0.1 mg/mL BSA, 100 μ M Na_3VO_4 , and 0.5 mM DTT). Recombinant activated human p38 enzyme (1 nM) was mixed with 50 μ M ATP and 100 nM GST-ATF2-Avitag, in the presence or absence of inhibitor. The reaction was allowed to incubate for 1 h at RT. The kinase reaction was terminated and phospho-ATF2 was revealed by addition of 30 μ L of HTRF detection buffer (100 mM HEPES-pH 7.5, 100 mM NaCl, 0.1% BSA, 0.05% Tween-20, and 10 mM EDTA) supplemented with 0.1 nM Eu-anti-pTP and 4 nM SA-APC. After 1 h incubation at RT, the assay plate was read in a Discovery Plate Reader (Perkin-Elmer). The wells were excited with coherent 320 nm light and the ratio of delayed (50 ms post excitation) emissions at 620 nm (native europium fluorescence) and 665 nm (europium fluorescence transferred to allophycocyanin – an index of substrate phosphorylation) was determined.¹⁹

LPS-Induced TNF α Production in THP-1 Cells. THP1 cells were resuspended in fresh THP1 media (RPMI 1640, 10% heat-inactivated FBS, 1 \times PGS, 1 \times NEAA, plus 30 μ M β ME) at a concentration of 1.5×10^6 cells per mL. One hundred microliters of cells per well were plated in a flat bottom polystyrene 96-well tissue culture plate. Two micrograms per milliliter of bacterial LPS (Sigma) was prepared in THP1 media and transferred to the first 11 columns of a 96-well polypropylene plate. Column 12 contained only THP1 media for the LO control. Compounds were dissolved in 100% DMSO and serially diluted 3-fold in a polypropylene 96-well microtiter plate (drug plate). Columns 6 and 12 were reserved as controls (HI control and LO control, respectively) and contained only DMSO. One microliter of inhibitor compound from the drug plate followed by 10 μ L of LPS was transferred to the cell plate. The treated cells were induced to synthesize and secrete TNF α in a 37 °C humidified incubator with 5% CO₂ for 3 h. TNF α production was determined by transferring 50 μ L of conditioned media to a 96-well small spot TNF α plate (MSD – Meso Scale Discovery) containing 100 μ L of 2 \times Read Buffer P supplemented with an anti-TNF α polyclonal Ab labeled with ruthenium (MSD-Sulfo-TAG – NHS ester). After overnight incubation at RT with shaking, the reaction was read on the Sector Imager 6000 (MSD). A low voltage was applied to the ruthenylated TNF α immune complexes, which in the presence of TPA (the active component in the ECL reaction buffer, Read Buffer P), resulted in a cyclical redox reaction generating light at 620 nm. The amount of secreted TNF α in the presence of compound compared with that in the presence of DMSO vehicle alone (HI control) was calculated using the formula: % control (POC) = (compd – average LO)/(average HI – average LO)*100.

TNF α -Challenged IL-8 Production in Human Whole Blood Cells. Whole blood was drawn from healthy, nonmedicated volunteers into sodium heparin tubes. 100 μ L of blood was then plated into 96-well tissue culture plates (BD). Ten point compound titrations were added to the blood and incubated for 1 h

at 37 °C with 5% CO₂. TNF α with a final concentration of 1 nM was then added to the blood and incubated overnight (16–18 h) at 37 °C with 5% CO₂. Plasma was harvested and cytokines (IL8) were measured by MSD (Meso Scale Discovery) ECL based antibody sandwich assay. All reagents were prepared in RPMI 1640, 10% v/v human serum AB (Gemini Bio-Products), 1 \times Pen/Strep/Glu. Final concentration of human whole blood was 50%. Data were analyzed using XLfit/Activity Base software package (IDBS).

Lipopolysaccharide (LPS)-Induced TNF Study. Lipopolysaccharide (Sigma Chemical Co.) was diluted in phosphate buffered saline (PBS, Life Technologies) to a concentration of 500 μ g/mL. The vehicle or compound **31** as a solution in 15% hydroxypropyl-cyclodextrin, 1% hydroxymethylcellulose, 1% Pluronic F68 was administered orally to female Lewis rats ($n = 6$) 1 h prior to injection with LPS (100 μ g/rat, iv, tail vein). Blood was harvested 90 min following the administration of LPS. Serum TNF α levels were analyzed using rat TNF α CytoSet kit from Biosource International. Data points represent the mean \pm SEM.

Collagen Induced Arthritis Model. Arthritis was induced by intradermal injection of Porcine type II collagen emulsified 1:1 in incomplete Freund's adjuvant (IFA). Animals were assigned to treatment groups at disease onset (study day 0), which occurred 10–12 days following immunization. Compound **31** or vehicle was administered orally once a day for 7 days. Paw diameter was measured daily from day 0 through day 7.

Area under the paw swelling curve (AUC) was calculated and used to determine percent inhibition of inflammation compared with vehicle controls. Data points represent the mean \pm SEM ($n = 8$ rats/group).

Acknowledgment. We thank Dr. Randy Jensen and Chris Wilde for providing NMR analyses. We also acknowledge all of our colleagues on the p38 MAP kinase research team.

References

- (1) (a) Chen, Z.; Gibson, T. B.; Robinson, F.; Silvestro, L.; Pearson, G.; Xu, B.; Wright, A.; Vanderbilt, C.; Cobb, M. H. MAP Kinases. *Chem. Rev.* **2001**, *101*, 2449–2476. (b) Pearson, G.; Robinson, F.; Gibson, T. B.; Xu, B.; Karandikar, M.; Berman, K.; Cobb, M. H. Mitogen-Activated Protein (MAP) Kinase Pathways: Regulation and Physiological Functions. *Endocr. Rev.* **2001**, *22*, 153–183.
- (2) (a) Lee, J. C.; Laydon, J. T.; McDonnell, P. C.; Gallagher, T. F.; Kumar, S.; Green, D.; McNulty, D.; Blumenthal, M. J.; Heys, J. R.; Landvatter, S. W.; Strickler, J. E.; McLaughlin, M. M.; Siemens, I. R.; Fisher, S. M.; Livi, G. P.; White, J. R.; Adams, J. L.; Young, P. R. A Protein Kinase Involved in the Regulation of Inflammatory Cytokine Biosynthesis. *Nature* **1994**, *372*, 739–746. (b) Jiang, Y.; Chen, C.; Li, Z.; Gegner, J. A.; Lin, S.; Han, J. Characterization of the Structure and Function of a New Mitogen-activated Protein Kinase (p38 β). *J. Biol. Chem.* **1996**, *271*, 17920–17926. (c) Kumar, S.; McDonnell, P. C.; Gum, R. J.; Hand, A. T.; Lee, J. C.; Young, P. R. Novel Homologues of CSBP/p38 MAP Kinase-Activation, Substrate Specificity and Sensitivity to Inhibition by Pyridinyl Imidazoles. *Biochem. Biophys. Res. Commun.* **1997**, *235*, 533–538. (d) Li, Z.; Jiang, Y.; Ulevitch, R. J.; Han, J. The Primary Structure of p38 γ : A New Member of p38 Group of MAP Kinases. *Biochem. Biophys. Res. Commun.* **1996**, *228*, 334–340. (e) Mertens, S.; Craxton, M.; Goedert, M. SAP Kinase-3, a New Member of the Family of Mammalian Stress-activated Protein Kinases. *FEBS Lett.* **1996**, *383*, 273–276. (f) Cuenda, A.; Cohen, P.; Buee-Scherrer, V.; Goedert, M. Activation of Stress-activated Protein Kinase-3 (SAPK3) by Cytokines and Cellular Stresses is Mediated via SAPKK3 (MKK6); Comparison of the Specificities of SAPK3 and SAPK2 (RK/p38). *EMBO J.* **1997**, *16*, 295–305.
- (3) (a) Ono, K.; Han, J. The p38 Signal Transduction Pathway Activation and Function. *Cell. Signal.* **2000**, *12*, 1–13. (b) Kumar, S.; Boehm, J.; Lee, J. C. p38 MAP Kinases: Key Signaling Molecules as Therapeutic Targets for Inflammatory Diseases. *Nat. Rev. Drug Discovery* **2003**, *2*, 717–726. (c) Saklatvala, J. The p38 MAP Kinase Pathway as a Therapeutic Target in Inflammatory Disease. *Curr. Opin. Pharmacol.* **2004**, *4*, 372–377.

- (4) Palladino, M. A.; Bahjat, F. R.; Theodorakis, E. A.; Moldawer, L. L. Anti-TNF- α Therapies: The Next Generation. *Nat. Rev. Drug Discovery* **2003**, *2*, 736–746.
- (5) (a) Goldstein, D. M.; Gabriel, T. Pathway to the Clinic: Inhibition of p38 MAP Kinase. A Review of Ten Chemotypes Selected for Development. *Curr. Top. Med. Chem.* **2005**, *5*, 1017–1029. (b) Hynes, J. Jr.; Leftheris, K. Small Molecule p38 Inhibitors: Novel Structural Features and Advances from 2002–2005. *Curr. Top. Med. Chem.* **2005**, *5*, 967–985. (c) Dominguez, C.; Tamayo, N.; Zhang, D. p38 Inhibitors: Beyond Pyridinylimidazoles. *Expert Opin. Ther. Pat.* **2005**, *15*, 801–816. (d) Peifer, C.; Wagner, G.; Laufer, S. New Approaches to the Treatment of Inflammatory Disorders Small Molecule Inhibitors of p38 MAP Kinase. *Curr. Top. Med. Chem.* **2006**, *6*, 113–149. (e) Pettus, L. H.; Wurz, R. P. Small Molecule p38 MAP Kinase Inhibitors for the Treatment of Inflammatory Diseases: Novel Structures and Developments During 2006–2008. *Curr. Top. Med. Chem.* **2008**, *8*, 1452–1467. (f) Goldstein, D. M.; Kuglstatter, A.; Lou, Y.; Soth, M. J. Selective p38 α Inhibitors Clinically Evaluated for the Treatment of Chronic Inflammatory Disorders. *J. Med. Chem.* **2010**, *53*, 2345–2353. For latest development, please see the following. (g) Cheeseright, T. J.; Holm, M.; Lehmann, F.; Luik, S.; Gottert, M.; Melville, J. L.; Laufer, S. Novel Lead Structures for p38 MAP Kinase via FieldScreen Virtual Screening. *J. Med. Chem.* **2009**, *52*, 4200–4209. (h) Lumeras, W.; Caturla, F.; Vidal, L.; Esteve, C.; Balague, C.; Orellana, A.; Dominguez, M.; Roca, R.; Huerta, J. M.; Godessart, N.; Vidal, B. Design, Synthesis, and Structure-Activity Relationships of Aminopyridine N-Oxides, A Novel Scaffold for the Potent and Selective Inhibition of p38 Mitogen Activated Protein Kinase. *J. Med. Chem.* **2009**, *52*, 5531–5545. (i) Aston, N. M.; Bamborough, P.; Buckton, J. B.; Edwards, C. D.; Holmes, D. S.; Jones, K. L.; Patel, V. K.; Smees, P. A.; Somers, D. O.; Vitulli, G.; Walker, A. L. p38 α Mitogen-Activated Protein Kinase Inhibitors: Optimization of a Series of Biphenylamides to Give a Molecule Suitable for Clinical Progression. *J. Med. Chem.* **2009**, *52*, 6257–6269. (j) Laufer, S.; Lehmann, F. Investigations of SCIO-469-like Compounds for the Inhibition of p38 MAP Kinase. *Bioorg. Med. Chem. Lett.* **2009**, *19*, 1461–1464. (k) Cirillo, P. F.; Hickey, E. R.; Moss, N.; Breitfelder, S.; Betageri, R.; Tazmeen, F.; Gaenzler, F.; Gilmore, T.; Goldberg, D. R.; Kamhi, V.; Kirrane, T.; Kroe, R. R.; Madwed, J.; Moriaki, M.; Netherton, M.; Pargellis, C. A.; Patel, U. R.; Qian, K. C.; Sharma, R.; Sun, S.; Swinamer, A.; Torcellini, C.; Takhashi, H.; Tsang, M.; Xing, Z. Discovery and Characterization of the N-Phenyl-N'-naphthylurea Class of p38 Kinase Inhibitors. *Bioorg. Med. Chem. Lett.* **2009**, *19*, 2386–2391. (l) Selness, S. R.; Devraj, R. V.; Monahan, J. B.; Boehm, T. L.; Walker, J. K.; Devadas, B.; Durley, R. C.; Kurumbail, R.; Shieh, H.; Xing, L.; Hepperle, M.; Rucker, P. V.; Jerome, K. D.; Benson, A. G.; Marruffo, L. D.; Madsen, H. M.; Hitchcock, J.; Owen, T. J.; Christie, L.; Promo, M. A.; Hickory, B. S.; Alvira, E.; Naing, W.; Blevis-Bal, R. Discovery of N-Substituted Pyridinones as Potent and Selective Inhibitors of p38 Kinase. *Bioorg. Med. Chem. Lett.* **2009**, *19*, 5851–5856. (m) Li, J.; Kaoud, T. S.; Laroche, C.; Dalby, K. N.; Kerwin, S. M. Synthesis and Biological Evaluation of p38 α Kinase-Targeting Diallylimidazoles. *Bioorg. Med. Chem. Lett.* **2009**, *19*, 6293–6297. (n) Jerome, K. D.; Rucker, P. V.; Xing, L.; Shieh, H. S.; Baldus, J. E.; Selness, S. R.; Letavic, M. A.; Braganza, J. F.; McClure, K. F. Continued Exploration of the Triazolopyridine Scaffold as a Platform for p38 MAP Kinase Inhibition. *Bioorg. Med. Chem. Lett.* **2010**, *20*, 469–473. (o) Mavunkel, B. J.; Perumattam, J. J.; Tan, X.; Leudtke, G. R.; Lu, Q.; Lim, D.; Kizer, D.; Dugar, S.; Chakravarty, S.; Xu, Y.-J.; Jung, J.; Liclican, A.; Levy, D. E.; Tabora, J. Piperidine-based Heterocyclic Oxalyl Amides as Potent p38 α MAP Kinase Inhibitors. *Bioorg. Med. Chem. Lett.* **2010**, *20*, 1059–1062. (p) Luedtke, G. R.; Schinzel, K.; Tan, X.; Tester, R. W.; Nashashibi, I.; Xu, Y.-J.; Dugar, S.; Levy, D. E.; Jung, J. Amide-based Inhibitors of p38 α MAP Kinase. Part 1: Discovery of Novel N-Pyridyl Amide Lead Molecules. *Bioorg. Med. Chem. Lett.* **2010**, *20*, 2556–2559. (q) Tester, R.; Tan, X.; Luedtke, G.; Nashashibi, I.; Schinzel, K.; Liang, W.; Jung, J.; Dugar, S.; Liclican, A.; Tabora, J.; Levy, D. E.; Do, S. Amide-based Inhibitors of p38 α MAP Kinase. Part 2: Design, Synthesis and SAR of Potent N-Pyrimidyl Amides. *Bioorg. Med. Chem. Lett.* **2010**, *20*, 2560–2563. (r) Walker, J. K.; Selness, S. R.; Devraj, R. V.; Hepperle, M. E.; Naing, W.; Shieh, H.; Kurumbail, R.; Yang, S.; Flynn, D. L.; Benson, A. G.; Messing, D. M.; Dice, T.; Kim, T.; Lindmark, R. J.; Monahan, J. B.; Portanova, J. Identification of SD-0006, a Potent Diaryl Pyrazole Inhibitor of p38 MAP Kinase. *Bioorg. Med. Chem. Lett.* **2010**, *20*, 2634–2638. (s) Tynebor, R. M.; Chen, M.-H.; Natarajan, S. R.; O'Neill, E. A.; Thompson, J. E.; Fitzgerald, C. E.; O'Keefe, S. J.; Doherty, J. B. Synthesis and Biological Activity of 2H-Quinolizin-2-one Based p38 α MAP Kinase Inhibitors. *Bioorg. Med. Chem. Lett.* **2010**, *20*, 2765–2769. (t) Dorn, A.; Schattel, V.; Laufer, S. Design, Synthesis and SAR of Phenylamino-substituted 5,11 dihydroadibenzof[a,d]cyclohept-10-ones and 11H-dibenzof[b,f]oxepin-10-ones as p38 MAP Kinase Inhibitors. *Bioorg. Med. Chem. Lett.* **2010**, *20*, 3074–3077. (u) Jerome, K. D.; Hepperle, M. E.; Walker, J. K.; Xing, L.; Devraj, R. V.; Benson, A. G.; Baldus, J. E.; Selness, S. R. Discovery of 5-Substituted-N-arylpyridazinones as Inhibitors of p38 MAP Kinase. *Bioorg. Med. Chem. Lett.* **2010**, *20*, 3146–3149.
- (6) (a) Herberich, B.; Cao, G.-Q.; Chakrabarti, P. P.; Falsey, J. R.; Pettus, L.; Rzaia, R. M.; Reed, A. B.; Reichelt, A.; Sham, K.; Thaman, M.; Wurz, R. P.; Xu, S.; Zhang, D.; Hsieh, F.; Lee, M. R.; Syed, R.; Li, V.; Grosfeld, D.; Plant, M. H.; Henkle, B.; Sherman, L.; Middleton, S.; Wong, L. M.; Tasker, A. S. Discovery of Highly Selective and Potent p38 Inhibitors Based on a Phthalazine Scaffold. *J. Med. Chem.* **2008**, *51*, 6271–6279. (b) Pettus, L. H.; Xu, S.; Cao, G.-Q.; Chakrabarti, P. P.; Rzaia, R. M.; Sham, K.; Wurz, R. P.; Zhang, D.; Middleton, S.; Henkle, B.; Plant, M. H.; Saris, C. J. M.; Sherman, L.; Wong, L. M.; Powers, D. A.; Tudor, Y.; Yu, V.; Lee, M. R.; Syed, R.; Hsieh, F.; Tasker, A. S. 3-Amino-7-phthalazinylbenzoisoxazoles as a Novel Class of Potent, Selective, and Orally Available Inhibitors of p38 α Mitogen-Activated Protein Kinase. *J. Med. Chem.* **2008**, *51*, 6280–6292. (c) Wurz, R. P.; Pettus, L. H.; Xu, S.; Henkle, B.; Sherman, L.; Plant, M.; Miner, K.; McBride, H. J.; Wong, L. M.; Saris, C. J. M.; Lee, M. R.; Chmait, S.; Mohr, C.; Hsieh, F.; Tasker, A. S. Part 1: Structure–Activity Relationship (SAR) Investigations of Fused Pyrazoles as Potent, Selective and Orally Available Inhibitors of p38 α Mitogen-Activated Protein Kinase. *Bioorg. Med. Chem. Lett.* **2009**, *19*, 4724–4728. (d) Wurz, R. P.; Pettus, L. H.; Henkle, B.; Sherman, L.; Plant, M.; Miner, K.; McBride, H. J.; Wong, L. M.; Saris, C. J. M.; Lee, M. R.; Chmait, S.; Mohr, C.; Hsieh, F.; Tasker, A. S. Part 2: Structure–Activity Relationship (SAR) Investigations of Fused Pyrazoles As Potent, Selective and Orally Available Inhibitors of p38 α Mitogen-Activated Protein Kinase. *Bioorg. Med. Chem. Lett.* **2010**, *20*, 1680–1684. (e) Pettus, L. H.; Wurz, R. P.; Xu, S.; Herberich, B.; Henkle, B.; Liu, Q.; McBride, H. J.; Mu, S.; Plant, M. H.; Saris, C. J. M.; Sherman, L.; Wong, L. M.; Chmait, S.; Lee, M. R.; Mohr, C.; Hsieh, F.; Tasker, A. S. Discovery and Evaluation of 7-Alkyl-1,5-bis-aryl-pyrazolopyridinones as Highly Potent, Selective, and Orally Efficacious Inhibitors of p38 α Mitogen-Activated Protein Kinase. *J. Med. Chem.* **2010**, *53*, 2973–2985.
- (7) For references comparing DFG-in and DFG-out binding, see the following: (a) Nagar, B.; Bornmann, W. G.; Pellicani, P.; Schindler, T.; Veach, D. R.; Miller, W. T.; Clarkson, B.; Kuriyan, J. Crystal Structures of the Kinase Domain of c-Abl in Complex with the Small Molecule Inhibitors PD17955 and Imatinib (STI-571). *Cancer Res.* **2002**, *62*, 4236–4243. (b) Tokarski, J. S.; Newitt, J. A.; Chang, C. Y. J.; Cheng, J. D.; Wittekind, M.; Kiefer, S. E.; Kish, K.; Lee, F. Y. F.; Borzilleri, R.; Lombardo, L. J.; Xie, D.; Zhang, Y.; Klei, H. E. The Structure of Dasatinib (BMS-354825) Bound to Activated ABL Kinase Domain Elucidates Its Inhibitory Activity against Imatinib-Resistant ABL Mutants. *Cancer Res.* **2006**, *66*, 5790–5797. (c) Zuccotto, F.; Ardini, E.; Casale, E.; Angiolini, M. Through the “Gatekeeper Door”: Exploiting the Active Kinase Conformation. *J. Med. Chem.* **2010**, *53*, 2681–2694.
- (8) Atomic coordinates and structure factors for crystal structures of compounds **1** and **2** bound to p38 α can be accessed using PDB codes 3DS6 and 3GFE, respectively.
- (9) Fitzgerald, C. E.; Patel, S. B.; Becker, J. W.; Cameron, P. M.; Zaller, D.; Pikounis, V. B.; O'Keefe, S. J.; Scapin, G. Structural Basis for p38 α MAP Kinase Quinazolinone and Pyridol-Pyrimidine Inhibitor Specificity. *Nat. Struct. Biol.* **2003**, *10*, 764–769.
- (10) Manning, G.; Whyte, D. B.; Martinez, R.; Hunter, T.; Sudarsanam, S. The Protein Kinase Complement of the Human Genome. *Science* **298**, 1912–1934.
- (11) (a) Pilgram, K. H.; Pollard, G. E. 4-(and 5)-Cyclopropylamino-5-(and 4)-halo-3(2H)pyridazinones. Formation and Characterization of Isomers. *J. Heterocycl. Chem.* **1977**, 1039–1043. (b) Lyga, J. W. The Reaction of 2-Substituted-4,5-dichloro-3(2H)-pyridazinones with Alkoxides and Alkylthiolates. *J. Heterocycl. Chem.* **1988**, 1757–1760. (c) Park, J.-W.; Yoon, Y.-J. Direct Functionalization of 4,5-Dichloropyridazin-6-one. *J. Heterocyclic Chem.* **1999**, 905–910.
- (12) Martinelli, J. R.; Freckmann, D. M. M.; Buchwald, S. L. Convenient Method for the Preparation of Weinreb Amides via Pd-Catalyzed Aminocarbonylation of Aryl Bromides at Atmospheric Pressure. *Org. Lett.* **2006**, *8*, 4843–4846.
- (13) Raitio, K. H.; Savinainen, J. R.; Vepsäläinen, J.; Laitinen, J. T.; Poso, A.; Jarvinen, T.; Nevalainen, T. Synthesis of SAR Studies of 2-Oxoquinoline Derivatives as CB2 Receptor Inverse Agonists. *J. Med. Chem.* **2006**, *49*, 2022–2027.
- (14) Chowdhury, S.; Roy, S. The First Example of a Catalytic Hunsdiecker Reaction: Synthesis of β -Halostyrenes. *J. Org. Chem.* **1997**, *62*, 199–200.
- (15) (a) Charles, M. D.; Schultz, P.; Buchwald, S. L. Efficient Pd-Catalyzed Amination of Heteroaryl Halides. *Org. Lett.* **2005**, *7*, 3965–3968. (b) Burgos, C. H.; Barder, T. E.; Huang, X.; Buchwald,

- S. L. Significantly Improved Method for the Pd-Catalyzed Coupling of Phenols with Aryl Halides: Understanding Ligand Effects. *Angew. Chem., Int. Ed.* **2006**, *45*, 4321–4326. (c) Chen, M.-H.; Doherty, J. B.; Tynebor, R. p38 Kinase Inhibiting Agents. US 2007129372 A1, 2007.
- (16) (a) Angell, R. M.; Baldwin, I. R.; Bamborough, P.; Deboeck, N. M.; Longstaff, T.; Swanson, S. Fused Heteroaryl Derivatives for Use as p38 Kinase Inhibitors in the Treatment of I. A. Rheumatoid Arthritis. WO 04010995 A1, 2004. (b) Bamborough, P.; Campos, S. A.; Patel, V. K.; Swanson, S.; Walker, A. L. Fused Heteroaryl Derivatives for Use as p38 Kinase Inhibitors. WO05073189 A2, 2005. (c) Tasker, A.; Zhang, D.; Cao, G.-Q.; Chakrabarti, P. P.; Falsey, R. J.; Herberich, B. J.; Hungate, R. W.; Pettus, L. H.; Reed, A.; Rzasa, R. M.; Sham, K. K. C.; Thaman, M. C.; Xu, S. Phthalazine, Aza- and Diaza-Phthalazine Compounds and Methods of Use. WO 06094187 A2, 2006. (d) Zhang, D.; Tasker, A. S.; Sham, K. K. C.; Chakrabarti, P. P.; Falsey, R. J.; Herberich, B. J.; Pettus, L. H.; Rzasa, R. M. Imidazo- and Triazolo-Pyridine Compounds and Methods of Use Thereof. WO08045393, 2008. (e) Pettus, L. H.; Tasker, A.; Xu, S.; Wurz, R. Pyrazolo-Pyridinone Compounds, Process for Their Preparation, and Their Pharmaceutical Use. WO08137176, 2008.
- (17) (a) Goldstein, D. M.; Alfredson, T.; Bertrand, J.; Browner, M. F.; Clifford, K.; Dalrymple, S. A.; Dunn, J.; Freire-Moar, J.; Harris, S.; Labadie, S. S.; La Fargue, J.; Lapierre, J. M.; Larrabee, S.; Li, F.; Papp, E.; McWeeney, D.; Ramesha, C.; Roberts, R.; Rotstein, D.; San Pablo, B.; Sjogren, E. B.; So, O.-Y.; Talamas, F. X.; Tao, W.; Trejo, A.; Villasenor, A.; Welch, M.; Welch, T.; Weller, P.; Whiteley, P. E.; Young, K.; Zipfel, S. Discovery of *S*-[5-Amino-1-(4-fluorophenyl)-1*H*-pyrazol-4-yl]-[3-(2,3 dihydroxypropoxy)-phenyl]methanone (RO3201195), an Orally Bioavailable and Highly Selective Inhibitor of p38 Map Kinase. *J. Med. Chem.* **2006**, *49*, 1562–1575. (b) Liu, C.; Wroblewski, S. T.; Lin, J.; Ahmed, G.; Metzger, A.; Wityak, J.; Gillooly, K. M.; Shuster, D. J.; McIntyre, K. W.; Pitt, S.; Shen, D. R.; Zhang, R. F.; Zhang, H.; Doweyko, A. M.; Diller, D.; Henderson, I.; Barrish, J. C.; Dodd, J. H.; Schieven, G. L.; Leftheris, K. 5-Cyanopyrimidine Derivatives as a Novel Class of Potent, Selective, and Orally Active Inhibitors of p38 α MAP Kinase. *J. Med. Chem.* **2005**, *48*, 6261–6270.
- (18) Assays were performed by Ambit Biosciences (San Diego, CA: <http://www.ambitbio.com/>) utilizing KINOMEscan. Activity is recorded via a competition binding assay of selected kinases that are fused to a proprietary tag. POC values are determined by measurements of the amount of kinase bound to an immobilized, active-site directed ligand in the presence and absence of the test compound. For more information on this method, see Fabian, M. A.; Biggs, W. H., III; Treiber, D. K.; Atteridge, C. E.; Azimioara, M. D.; Benedetti, M. G.; Carter, T. A.; Ciceri, P.; Edeen, P. T.; Floyd, M.; Ford, J. M.; Galvin, M.; Gerlach, J. L.; Grotzfeld, R. M.; Herrgard, S.; Insko, D. E.; Insko, M. A.; Lai, A. G.; Lélias, J.-M.; Mehta, S. A.; Milanov, Z. V.; Velasco, A. M.; Wodicka, L. M.; Patel, H. K.; Zarrinkar, P. P.; Lockhart, D. J. A. Small Molecule-Kinase Interaction Map for Clinical Kinase Inhibitors. *Nat. Biotechnol.* **2005**, *23*, 329–336.
- (19) Park, Y.-W.; Cummings, R. T.; Wu, L.; Zheng, S.; Cameron, P. M.; Woods, A.; Zaller, D. M.; Marcy, A. I.; Hermes, J. D. Homogeneous Proximity Tyrosine Kinase Assays: Scintillation Proximity Assay versus Homogeneous Time-Resolved Fluorescence. *Anal. Biochem.* **1999**, *269*, 94–104.